Cement and Concrete Composites 133 (2022) 104721

Contents lists available at ScienceDirect

Cement and Concrete Composites

journal homepage: www.elsevier.com/locate/cemconcomp

# Estimating compressive strength of lightweight foamed concrete using neural, genetic and ensemble machine learning approaches

Babatunde Abiodun Salami [a], Mudassir Iqbal [c], Abdulazeez Abdulraheem [d], Fazal E. Jalal [b], Wasiu Alimi [e], Arshad Jamal [f], T. Tafsirojjaman [g,h], Yue Liu [i,*], Abidhan Bardhan [j]

[a] *Interdisciplinary Research Center for Construction and Building Materials, Research Institute, King Fahd University of Petroleum and Minerals, Dhahran, 31261, Saudi Arabia*
[b] *Department of Civil Engineering, University of Engineering and Technology Peshawar, Pakistan*
[c] *Shanghai Key Laboratory for Digital Maintenance of Buildings and Infrastructure, State Key Laboratory of Ocean Engineering, School of Naval Architecture, Ocean & Civil Engineering, Shanghai Jiao Tong University, Shanghai, 200240, China*
[d] *College of Petroleum Engineering & Geosciences, King Fahd University of Petroleum & Minerals, Dhahran, 31261, Saudi Arabia*
[e] *Civil and Environmental Engineering Department, College of Engineering, King Fahd University of Petroleum and Minerals, Dammam, 31261, Saudi Arabia*
[f] *Transportation and Traffic Engineering Department, College of Engineering, Imam Abdulrahman Bin Faisal University, P.O. Box 1982, Dammam, 31451, Saudi Arabia*
[g] *School of Civil, Environmental and Mining Engineering, The University of Adelaide, Adelaide, Australia*
[h] *Centre for Future Materials (CFM), School of Engineering, University of Southern Queensland (USQ), Toowoomba, QLD, 4350, Australia*
[i] *Research Institute of Urbanization and Urban Safety, University of Science and Technology Beijing, 30 Xueyuan Road, Beijing, China*
[j] *Civil Engineering Department, National Institute of Technology (NIT) Patna, India*

A R T I C L E I N F O

*Keywords:*
Foamed concrete
Lightweight concrete
Artificial neural network
Gene expression programming
Gradient boosting tree
Optimization

A B S T R A C T

Foamed concrete is special not only in terms of its unique properties, but also in terms of its challenging compositional mixture design, which necessitates multiple experimental trials before obtaining the desired property like compressive strength. Regardless of design challenges, artificial intelligence (AI) techniques have shown to be useful in reliably estimating desired concrete properties based on optimized mixture proportions. This study proposes AI-based models to predict the compressive strength of foamed concrete. Three novel AI approaches, namely artificial neural network (ANN), gene expression programming (GEP), and gradient boosting tree (GBT) models, were employed. The models were developed using 232 experimental results, considering easily acquired variables, such as the density of concrete, water-cement ratio and sand-cement ratio as inputs to estimate the compressive strength of foamed concrete. In training the models, 80% of the experimental data was used and the rest was used to validate the models. The optimized models were selected using their respective best hyper-parameters on trial and error basis; variable number of hidden layers, number of neurons and training algorithms were used for ANN, number of chromosomes, head size, number of genes, variable function set for the GEP and GBT employed number of trees, maximal depth and learning rate. The trained models were validated using parametric and sensitivity analyses of a simulated dataset. The prediction abilities of proposed models were evaluated using the coefficient of correlation (R), mean absolute error (MAE), and root mean squared error (RMSE). For the validation data, empirical results from the performance evaluation revealed that GBT model (R = 0.977, MAE = 1.817 and RMSE = 2.69) has relative superior performance with highest correlation and least error in comparison with ANN (R = 0.975, MAE = 2.695 and RMSE = 3.40) and GEP (R = 0.96, MAE = 2.07 and RMSE = 2.80). The study concludes that the developed GBT model offered reliable accuracy in predicting the compressive strength of foamed concrete. Finally, the simple prediction equation generated from the GEP model signifies its importance and can reliably be used in estimating compressive strength of foamed concrete. It is recommended that the prediction models shall be used for the ranges of input variables employed in this study.

* Corresponding author.
*E-mail address:* yueliu@ustb.edu.cn (Y. Liu).

https://doi.org/10.1016/j.cemconcomp.2022.104721
Received 28 January 2022; Received in revised form 1 July 2022; Accepted 9 August 2022
Available online 21 August 2022

## 1. Introduction

Concrete is a widely used construction material in reinforced concrete structures, owing to its better composite behavior with steel. The ingredients of concrete are replaced (partially or completely) by a variety of substitutes to change its mechanical and durability properties [1,2]. Foamed concrete (FC) is a light cellular concrete that resembles the lightweight (LW) concrete (density ranges between 300 and 1850 kg/m$^3$) [3] with randomly enclosed air voids in the binding mortar, which is responsible for its reduced self-weight [4]. The FCs are known by other names, such as, low-density FC, cellular LW concrete, and LW cellular concrete [5–8]. Note that the FC material is by no means a new product but has gained popularity in recent years because of its cost-effectiveness and sustainable alternative to the traditional concrete [9]. They have been used to build earthquakes and fire resistant LW structures [10,11]. FC comprises cement, fine and coarse aggregates, water and foaming agents, which imparts the "LW behaviour" to the concrete. In addition to the aforementioned traditional ingredients, many researchers have introduced binder supplements, such as, glass and rubber waste from industries [12,13], eggshell waste [14–16] and sawdust [17]. These supplementary materials act as "diets" for the FC, positioning it as a solution to some of the environmental and economic issues, in addition to properties enhancement [18]. These properties are influenced by various characteristics of the constituent materials (i.e., foaming agent type, cement minerology, and aggregate granulometry), pore nature and uniformity, water quality, mixture proportion of the materials and the adopted curing methods [19]. Ordinarily, a higher compressive strength is synonymous with higher cement content, as reported for normal concrete [20]. A similar trend can be observed in the case of FCs; however, a decrease in strength is observed when the cement content exceeds 500 kg/m$^3$ [21]. In addition, a greener FC was achieved through partial replacement of cement by supplementary cementitious materials [22].

The LW nature of typical FC is a result of presence of air bubbles from a mixture of water, foaming chemicals and pressurized air [3]. Commonly available foaming agents are detergents, glue resins, hydrolyzed proteins, protein-based resin soap, saponins and synthetic agents, such that the synthetic and protein-based foaming agents are most commonly utilized [23,24]. In order to obtain a particular property of foamed concrete practically, there is no specific mixture proportioning procedure available. However, several trial and error sessions are usually conducted to determine the optimal mixture using metrics, such as, binder content, percentage foam content, and net water content [23,25]. With the appropriate blend of mixtures, FCs exhibit superior qualities, for instance high strength-to-weight ratio and low density, which assist in minimizing the dead loads, foundation size as well as the construction costs pertaining to labor, material transport, and operation [26–28]. Besides, owing to their textured surface and cellular microstructure the FCs are resistant to fire, good thermal conductivity, balanced energy conservation and enhanced sound adsorption [4,29]. FCs exhibition of several high-level and distinct properties, particularly density reduction, makes them environmentally friendly LW structural material in building and road construction projects. In comparison to other LW structural materials, such as dry walls and wood, FC is favourable in terms of the inherent environmental difficulties involved in their production process, alongside their high costs.

Low density and thermal conductivity as well as cost-effectiveness are some of the vital properties that have led to increased usage of FCs in myriad of civil infrastructural and structural applications [30,31]. Examples include the insulation and filling of cavities, LW precast concrete panels and blocks, insulation against fire, sound and heat, soil stabilization, shock-absorbing barriers for airports, and normal road traffic [30–34]. The impressive rheology of the FCs makes them viable choice for void filling, particularly in collapsing sewers, ducts, and voids beneath roadways [33]. Furthermore, the popularity of FCs has grown globally, with particular interest in areas experiencing shortage of houses or extreme weather conditions. Large quantities of FCs are consumed annually in developed and developing nations of the world, such as the UK (250,000–300,000 m$^3$), western Canada (~50,000 m$^3$), and Korea (250,000 m$^3$), to address issues related to load reduction, thermal insulation, structural stability, temperature changes, floor heating systems, and the expenses of repair and maintenance [33,35–38]. In building design, the structural loads (dead, live, wind, etc.) need to be resisted hence making them critical factors for consideration. The last few decades have witnessed construction of substantial number of large-scale tall buildings around the globe [39] wherein the reduction of structural loads is a recurring issue amongst designers and practitioners. From a structural material standpoint, balancing the strength requirements of the LW concrete for structural applications, for example LW blocks and precast panels, is a growing challenge that requires engineering solutions [29,40].

One of the most important characteristics of FC is its compressive strength since it gives an indication of its capacity to resist loads prior to failure. This further underscore the importance of the compressive strength characteristic. The density of FC has direct influence on its compressive strength through the performance characteristics of its constituents. A direct linear relationship exists between the compressive strength and density of the FC [41]. This relationship is shared by flexural and tensile strengths; as the density of the FC decreases, other properties, for instance, its durability performance [42–44], pore structural properties [45,46], fracture properties, [47] and other mechanical strength properties, [48–51], tend to decrease. The key parameters affecting the strength properties of the FCs include the water-to-binder ratio, sand-to-binder ratio, curing period, void distribution, and the type of foaming agent [52]. With the inclusion of additives and admixtures, the compressive strength properties were affected, and other parameters, such as the percentage of additive replacement for cement, dosage of admixtures, and air void size and shape (void structure), served as additional factors [53,54].

Several studies in the past attempted to estimate the compressive strength of the FCs by optimizing their constituents for performance enhancement. For example, the influence of mixture constituents on the compressive strength of FC was represented using Feret's formula [55,56], as shown in Eq. (1).

$$f_{cc} = k\left(\frac{1}{1+\frac{w}{c}+\frac{a}{c}}\right)^{m} \quad \text{Eq. 1}$$

where ($f_{cc}$) is the compressive strength, ($\frac{w}{c}$) is the water-cement ratio and ($\frac{a}{c}$) is the air-to-cement ratio. $k$ and $m$ are constants.

Other parameters considered in predicting the compressive strength of FC included porosity [56], compressive strength of the cement paste ($f_c$) [57], air content ($A$), and binder ratio ($\propto_b$) [51]. Pan et al. [50] proposed Eq. (2) and Eq. (3), which depict the relationships between the water-to-cement ratio ($\frac{w}{c}$), curing time ($t$) and compressive strength of the cement paste ($f_c$).

$$f_{cc} = 1.048 f_c (1-A)^{2.793} \quad \text{Eq. 2}$$

$$f_c = 88.04 + 6.569\ln(t) - \frac{130.5w}{c} \quad \text{Eq. 3}$$

In addition, Kearsley and Wainwright [51] derived the relationship between $\propto_b$, $f_c$ and $f_{cc}$ from Eq. (4).

$$f_{cc} = 1.172 f_c \propto_b^{3.7} \quad \text{Eq. 4}$$

They also performed regression analysis to establish another relationship to estimate the compressive strength using the dry density ratio ($\propto_d$) (Eq. (5)).

$$f_{cc} = f_c(-0.324 + 1.325\propto_d)^2 \quad \text{Eq. 5}$$

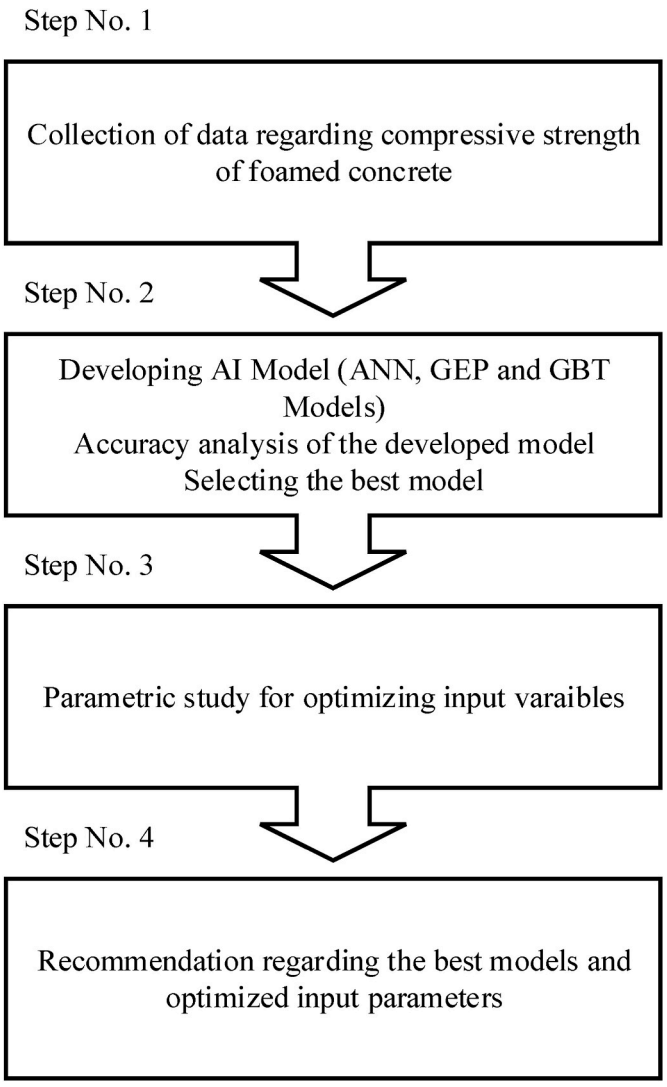


**Fig. 1.** Adopted methodology for the current research to evaluate the compressive strength of foamed concrete.

Previous empirical models that predicted the compressive strength of FCs mainly relied on foundational models such as Balshin's, Feret's, and Power's models [20]. Balshin's model relates the compressive strength of FC to the volume of voids present in concrete. Feret's model relates the compressive strength of the FC to the absolute volume of the constituent, whereas Power's model relates the strength to the gel-space ratio [58]. Detailed derivations of these empirical models are available in the published literature [59]. Most of the empirical models to forecast the compressive strength of FCs are calibrated using experimental data, which incorporates limited number of input parameters for developing the equations, making their predictions mostly extrapolative [60]. Note that prediction using an empirical model requires various constants that are not easily determinable while describing the complex relationship between the mixture proportions and the compressive strength [61].

Particularly, complexities exist in the design of FC mixture towards achieving a target or required compressive strength; for instance, there are reports that have revealed clear differences in the compressive strength between the protein-based foam agent and synthetic foam agent such that the former tends to have higher influence [62,63]. In addition, the production of air bubbles from the foaming agents has a substantial impact on numerous mechanical properties in contrast to others. Furthermore, the air bubbles have a greater influence on the compressive strength of FC than its modulus of elasticity which can be attributed to the higher stability of the foaming agent during blending [64]. It is pertinent to mention that deploying empirical and numerical techniques to model these complexities would be difficult, and the resulting models may not be suitable to estimate the intended targets with reasonable degree of accuracy. Currently, early decisions on the FC mixture design to accurately achieve a particular compressive strength are the most important requirement in the LW concrete research. This calls for the implementation of more powerful and advanced prediction tools such as machine learning (ML) algorithms. The ML algorithms have built-in capabilities to handle the complexities inherent in the FC mixture proportioning, which usually prevent the empirical equations from accurate prediction of the required concrete properties [65]. Also, the ML algorithms provide better predictions than those developed using traditional methods, such as trial-and-error or mathematical modelling, which are limited by human knowledge of physics. These techniques have become an essential part of civil and structural engineering for analytics and predictions [66–70]. A significant amount of current research is aimed at using ML for predictive modelling to design and predict the compressive strength of different types of concrete prior to casting, which would substantially reduce waste from laboratory trials before reaching optimum mixtures [66,71–73]. These algorithms have also been used to model the behaviour of concrete structures under different conditions [74]. As for the case of FCs, owing to the additional influencing variables, such as LW aggregate types, its mixture proportioning design can be challenging in laboratory experiments, especially because it mainly involves trial and error.

In a recent study by Zhang et al. [75], multi-objective optimization (MOO) was performed using least-squares support vector regression (LSSVR), in which hyperparameter tuning was performed using the firefly algorithm (FFA). Optimal FC mixtures using the proposed algorithms with high prediction accuracy and extremely minimal error were recorded, which allowed for early decision-making on the mixtures before casting. The compressive strength of FCs was estimated using the Levenberg – Marquardt-based artificial neural network (LM-ANN) approach, the parameters of which were optimized using particle swarm optimization (PSO) for achieving higher accuracy in the predictions. Using 375 experimental data points, including the dry density, w/c ratio, foam volume, sand/cement ratio, and testing age, the compressive strength of the FCs was predicted using the proposed PSO-LM-ANN hybrid algorithm [18]. In another deployment of the hybrid ML algorithm [76], the LSSVR with grey wolf optimization (GWO) algorithm was used to predict the compressive strength of the FCs. The results were compared with those of four other ML algorithms: support vector regression (SVR), random forest (RF), ANN and M5Rules. The performance of the hybrid algorithm (GWO-LSSVR) revealed that the predicted results were in good agreement with the actual values, with a correlation coefficient of 0.991 and MAPE of 0.0354, making the proposed algorithm an excellent tool for the mixture design of the FC. In yet another study, a conventional ANN (C-ANN) was proposed to predict the 28-day compressive strength of the FCs [77]. The network structure of the C-ANN was optimized, despite it being one of the most efficient ML algorithms for enhancing the prediction accuracy of the FC strength. The convergence of the predicted results was verified using a Monte Carlo simulation (MCS) with partial dependence plots (PDPs) of over 1000. MCS was used to interpret the relationship between the input variables (density, water/cement ratio and sand/cement ratio) and 28-day compressive strength. In addition, a deep neural network (DNN) with a novel higher-order neuron was developed to predict the compressive strength of the FCs. To enhance the model, the authors deployed a powerful entropy cost function and a rectified linear activation function. The results from the DNN models were compared with those of other ML algorithms [C-ANN and second-order ANN (SO-ANN)] to establish a genuine performance improvement with 1 or 2 hidden layers. An extreme learning machine (ELM) was used to predict the compressive strength of the FC [58]. To improve the performance of ELM, its

**Table 1**
Description of input and target parameters for model development.

| | Variable | Description | Unit | Max | Min | Standard deviation | Range |
|---|---|---|---|---|---|---|---|
| **Input** | Density | Density of concrete | $Kg/m^3$ | 2065.60 | 430.00 | 417.71 | 1635.60 |
| | w/c | Water to cement ratio | – | 0.83 | 0.26 | 0.13 | 0.57 |
| | s/c | Sand to cement ratio | – | 4.29 | 0.00 | 0.72 | 4.29 |
| **Target** | CS | Compressive strength | MPa | 51.18 | 1.50 | 13.93 | 49.68 |

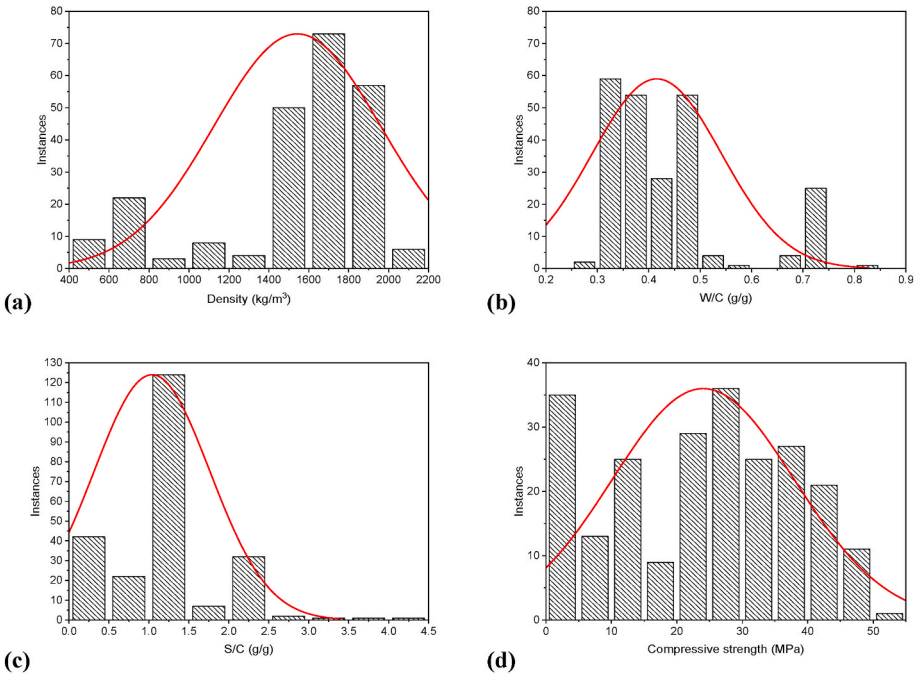


**Fig. 2.** Distribution histograms of the input and output variables used in the study.

**Table 2**
Linear Pearson's correlation between inputs and the target variable.

| Attribute | Compressive strength | Density | S/C | W/C |
|---|---|---|---|---|
| Compressive strength | 1.000 | 0.879 | 0.023 | −0.587 |
| Density | 0.879 | 1.000 | 0.328 | −0.517 |
| S/C | 0.023 | 0.328 | 1.000 | −0.068 |
| W/C | −0.587 | −0.517 | −0.068 | 1.000 |

**Table 3**
Setting parameter for ANN model.

| Parameter | Setting |
|---|---|
| Sampling | |
| Training record | 186 |
| Validation/testing | 46 |
| General | |
| Number of hidden layers | 01 |
| Number of hidden neurons | 10 |
| Fitness function | Mean squared error |
| Training Algorithm | Levenberg-Marquardt |
| Data division | Random |

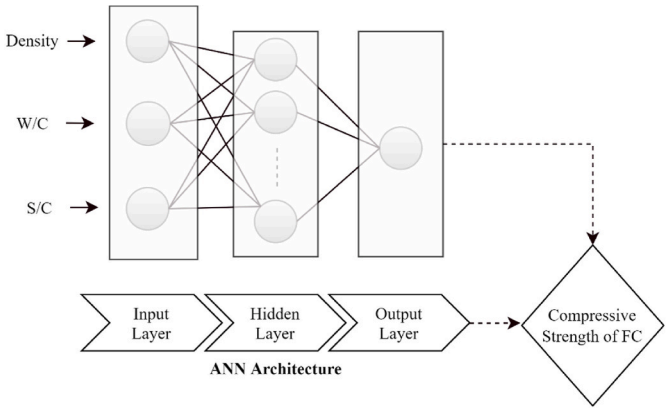


**Fig. 3.** The architecture of proposed ANN model to evaluate the compression strength of Foamed concrete.

prediction values were compared with those of other ML algorithms (multivariate adaptive regression spline (MARS), M5Tree, and SVR). With a better statistical score, the ELM model proved to be a reliable and accurate estimator for predicting the FC compressive strength.

The majority of past studies have focused on the use of neural networks with different architectures and optimization techniques based on SVM, ELM, MARS, etc., to estimate the compressive strength of various FCs. Most of the studies reported the performance of the prediction models without evaluating new data based on the developed models for the optimization of input variables. Besides, there is a need to expand on and show the capabilities of other techniques, especially new evolutionary paradigms such as gene expression programming (GEP) and ensemble models such as gradient boost tree (GBT) to accurately predict the properties of the FCs. In this study, the compressive strength is predicted using the strong nonlinear capabilities of three powerful ML algorithms: ANN, GEP, and GBT. Parametric Analysis has been carried out in order to optimize the water-cement ratio and sand-cement ratio

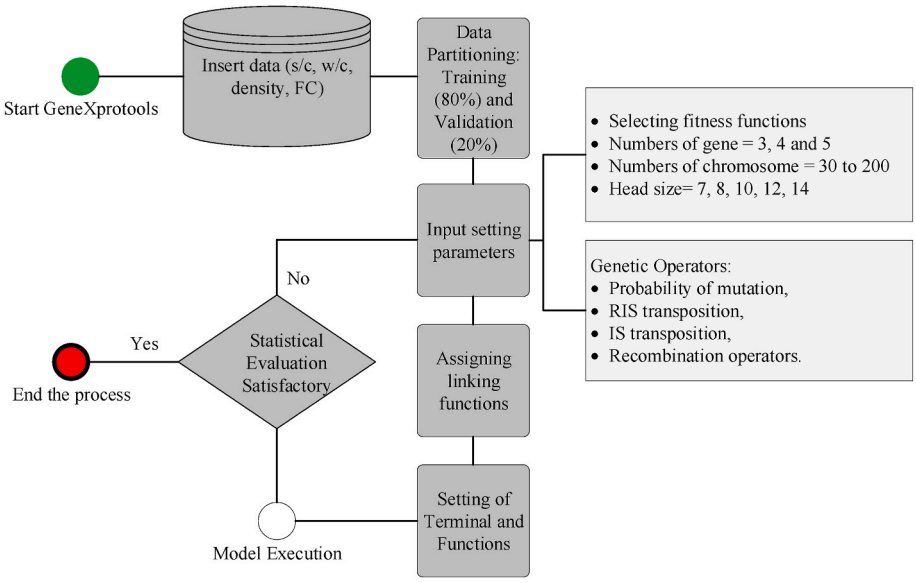


**Fig. 4.** GEP Prediction modelling of compression strength of Foamed concrete using GeneXProtools

**Table 4**
Statistical evaluation of the developed multiple models based on variable setting parameters.

| Variable setting parameters | | | Training data set | | | | Validation data set | | | |
|---|---|---|---|---|---|---|---|---|---|---|
| Model No. | Fitness function | Number of chromosomes, head size, genes | Correlation (R) | RMSE | MAE | RSE | Correlation (R) | RMSE | MAE | RSE |
| GEP1 | RMSE | 30, 7, 3 | 0.963 | 3.818 | 3.040 | 0.072 | 0.947 | 4.054 | 3.417 | 0.103 |
| GEP2 | RMSE | 30,8,3 | 0.954 | 4.093 | 3.353 | 0.090 | 0.961 | 4.204 | 3.516 | 0.080 |
| GEP3 | RMSE | 50,10,4 | 0.957 | 3.997 | 3.253 | 0.085 | 0.961 | 4.242 | 3.563 | 0.082 |
| **GEP4** | **RMSE** | **200,12,5** | **0.971** | **3.238** | **2.751** | **0.056** | **0.951** | **3.401** | **2.695** | **0.052** |
| GEP5 | RMSE | 200,14,5 | 0.940 | 3.706 | 3.706 | 0.116 | 0.936 | 5.318 | 4.252 | 0.128 |

**Table 5**
Setting parameter for optimized GEP model.

| Parameter | Setting |
|---|---|
| Sampling | |
| Training record | 186 |
| Validation/testing | 46 |
| General | |
| Genes | 3, 4,5 |
| Number of chromosomes | 30, 50, 100, 200 |
| Head size | 7,8, 10, 12,14 |
| Linking function | Addition |
| Function set | +,-,*,/,x^(1/3),x^2, |
| Numerical constants | |
| Constants per gene | 10 |
| Data type | Floating number |
| Upper bound | 10 |
| Lower bound | −10 |
| Genetic operators | |
| Mutation rate | 0.00138 |
| Fixed root mutation rate | 0.00068 |
| Function insertion rate | 0.00206 |
| Inversion rate | 0.00546 |
| IS transposition rate | 0.00546 |
| RIS transposition rate | 0.00546 |
| Gene composition rate | 0.00277 |
| Gene transposition rate | 0.00277 |

for specified density. A brief introduction to the problem is followed by the experimental database used in the development of the models, rationalization of the selected variables, brief description of the employed AI models, and prediction modelling. The results and discussion are provided in Section 3, which demonstrate the performance of the developed models and parametric as well as sensitivity analyses of each contributing variable. Finally, the major conclusions of this study are presented. The proposed models would be utilized in the selection of the appropriate mixture design choice for foamed concrete in order to achieve the requisite compressive strength as required by applications.

## 2. Research methodology

Fig. 1 shows the methodology adopted for the current research. The data was collected regarding the compressive strength of foamed concrete, which was used for developing AI models. ANN, GEP and GBT models were employed owing to its superior non-linear capabilities reported in the previous studies [78–80]. The methodology adopted in this study has been previously adopted by Iqbal et al. [81]. The developed models were assessed to select a more robust model, which was subsequently used for parametric analysis to optimize input parameters. A brief introduction of AI models and experimental database is presented herein. The detailed AI modeling is also explained in this section.

### 2.1. Experimental database

To develop a strong machine-learning model, it is critical to generate a well-constructed and extensive database, a clear and precise description of the database, statistically evaluated input variables, and insights into the datasets. Consequently, a database of cleaned data consisting of 232 foamed concrete experimental test results was developed from international publications by different researchers [82–87] as given as **supplementary data** was used to train the three algorithms selected for this study. The dataset is for different foamed concrete mixtures with density, water-to-cement (w/c) ratio and sand-to-cement (s/c) ratio as the input parameters and compressive strength (CS) as the output parameter. The input and target parameters (experimental design

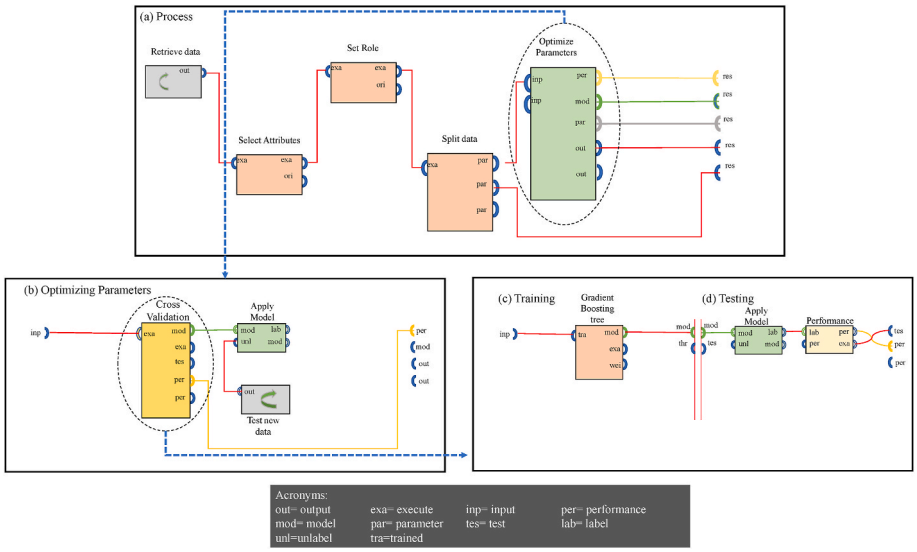


**Fig. 5.** Flow diagram depicting GBT modelling (Adapted from Iqbal et al. [81]).

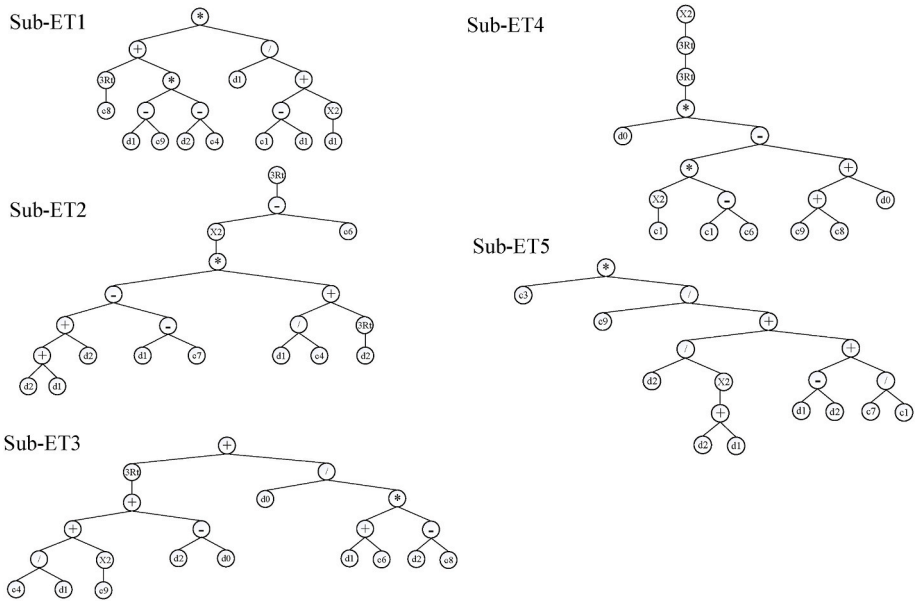


**Fig. 6.** Expression trees obtained from GEP4 model used in the development of mathematical equation.

variables) used in the study are listed in Table 1. Fig. 2 shows the distribution of the input and target parameters during the model development. These graphs are particularly valuable because they can assist in identifying parameter values for which data are insufficient and more data are required [88]. It can be seen that most of the datapoints manifest the density in between 1400 and 2000 kg/m$^3$ (Fig. 2a), w/c ratio (0.3–0.5) (Fig. 2b), and s/c ratio (0.5–2.0) (Fig. 2c). It is recommended that the developed models should be used within these input limits. Because the input parameters are interdependent, the correlation coefficients between all variables studied were calculated and are listed in Table 2. A brief examination of the connections between the input variables indicated that the density was strongly positive, and the w/c ratio showed a strong negative correlation with the compressive strength. The sand-to-cement ratio (s/c) exhibited a moderate negative correlation with the compressive strength of the foam concrete. The existence of correlations establishes a clear relationship between the input and target features, which allows the proposed techniques to learn these relationships easily and efficiently, leading to accurate prediction of the compressive strength.

### 2.2. Rationalization of the input parameters

Similar to any type of concrete, the properties of foamed concrete rely on the material properties and proportion of the mixture design to optimize its mechanical properties. In terms of the mechanical performance, the compressive strength of foamed concrete is the most important characteristic. Several studies have demonstrated that the compressive strength of foamed concrete decreases as its density increases. Owing to the high volume of voids within the microstructure of FC, the density decreases, which leads to a lower compressive strength. The effects of the properties and proportions of the power material on the properties of the FC were carefully studied and reviewed based on the available literature. Several studies [89,90] have reported a direct relationship between the density of the developed FC and its compressive strength. This relationship is established because FC is preferred as a building material because of its low density. FCs with densities ranging

**Table 6**
Optimization of GBT model.

| Model | Parameter | Value | Error rate optimization (%) |
|---|---|---|---|
| GBT | Number of trees, maximum depth, Learning rate | 30,2,0.001 | 40.95 |
| | | 90,2,0.001 | 39.82 |
| | | 150,2,0.001 | 38.72 |
| | | 30,4,0.001 | 40.93 |
| | | 90,4,0.001 | 39.77 |
| | | 150,4,0.001 | 38.65 |
| | | 30,7,0.001 | 40.93 |
| | | 90,7,0.001 | 39.77 |
| | | 150,7,0.001 | 38.65 |
| | | 30,2,0.01 | 36.39 |
| | | 90,2,0.01 | 29.00 |
| | | 150,2,0.01 | 24.49 |
| | | 30,4,0.01 | 36.09 |
| | | 90,4,0.01 | 28.07 |
| | | 150,4,0.01 | 23.10 |
| | | 30,7,0.01 | 36.09 |
| | | 90,7,0.01 | 28.07 |
| | | 150,7,0.01 | 23.10 |
| | | 30,2,0.1 | 16.57 |
| | | 90,2,0.1 | 15.58 |
| | | 150,2,0.1 | 15.52 |
| | | 30,4,0.1 | 15.85 |
| | | 90,4,0.1 | 13.59 |
| | | 150,4,0.1 | 13.58 |
| | | 30,7,0.1 | 15.81 |
| | | **90,7,0.1** | **13.45** |
| | | 150,7,0.1 | 13.53 |

from 400 to 1600 kg/m$^3$ have a strength of 1–10 MPa, which fill voids, stabilize structures, provide insulation, backfill bridge abutments, insulate slabs and houses, and has other subterranean uses [91]. Another important mixture design parameter that influences the compressive strength of FCs is the water/cement (w/c) ratio, whose optimum range for mortar and paste has been reported to be between 0.5 and 0.6. However, with the introduction of a superplasticizer, the water demand decreases, resulting in an optimum w/c between 0.17 and 0.19 [91]. A notable impact of the w/c ratio on the compressive strength of FC has also been reported in other studies, [92,93] because it ensures impressive paste fluidity and, as a result, leads to an even distribution of foam, thereby leading to strength growth. With the sand/cement (s/c) ratio, its relationship with the compressive strength of FC is inversely proportional. The amount of sand in foamed concrete determines its compressive strength, whereas the amount of foam added determines its density. Thus, FC's sand content requires comprehensive optimization in order to reach maximum effectiveness and ensure sufficient mix strength without sacrificing the intended purposes both economically as well as practical considerations of placing such concrete [94].

### 2.3. Adopted algorithms

To evaluate the compressive strength capacity of the foamed concrete, this study employed artificial neural networks (ANNs), gene expression programming (GEP), and gradient boost trees (GBT). This section provides a high-level overview of the machine-learning modelling strategies used in this study.

#### 2.3.1. Gradient boosted trees (GBT)

An ensemble of regression or classification tree models comprises a gradient-boosted tree (GBT) model. These are forward-learning ensemble approaches that provide predicted results by steadily improving estimates. Boosting is a robust nonlinear regression approach for enhancing tree accuracy. A series of decision trees are produced by progressively applying weak classification algorithms to gradually changing data, resulting in an ensemble of weak prediction models. While increasing the number of trees improves their accuracy, it also

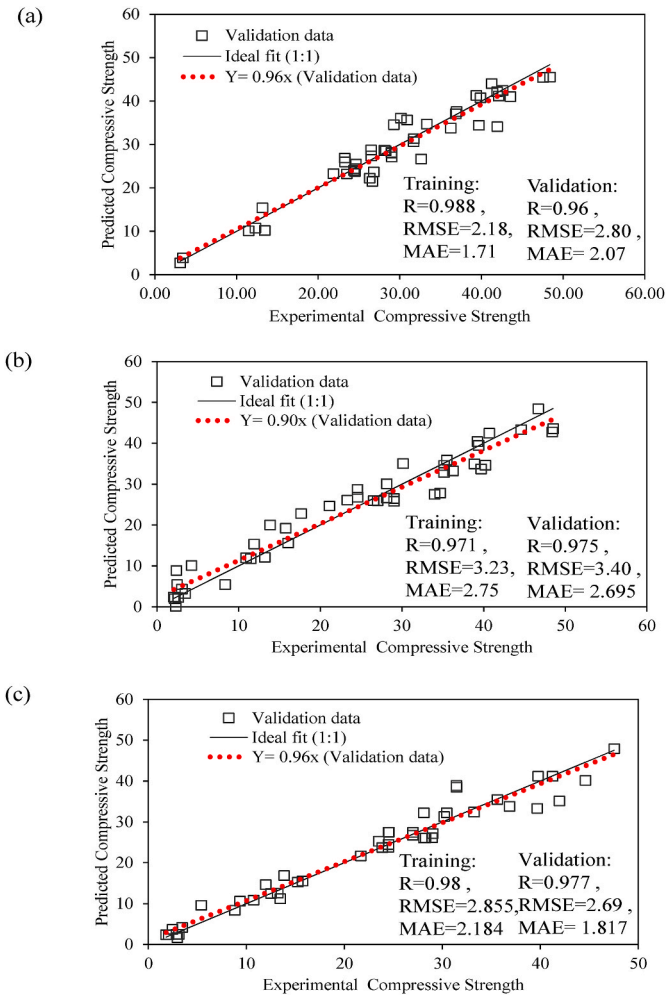


**Fig. 7.** Comparison of experimental and predicted results (a) ANN (b) GEP (c) GBT.

slows it down and makes it more difficult for humans to understand. To address these problems, the gradient boosting approach generalizes the tree boosting. GBT combines a series of weak base classifiers into a strong classifier. As opposed to traditional methods that consider both positive and negative sample weights, GBT achieves global convergence of the algorithm by following the direction of classification.

Let the dataset for training be $\{x_i, y_i\}_{i=1}^{n}$ with an N-dimensional vector of real values passed to the SoftMax function and in turn, produce an N-dimensional vector with real values of (0, 1), which sum to 1. To ensure convergence of the GBT model, a gradient descent algorithm is deployed to follow the direction of the negative gradient. The weak base learner is represented by $h(x)$, where $x_i = (x_{1i}, x_{2i}, \ldots, x_{qi})$, $q$ is the number of predicted parameters and $y_i$ is the predicted parameter. The step-by-step procedure followed by the GBT model for training the datasets is as follows:

(A) Using Eq. (6), the primary constant value (α) of the model was determined.

$$f(x) = \underset{\alpha}{\operatorname{argmin}} \sum_{i=1}^{N} L(y_i, \alpha) \qquad \text{Eq. 6}$$

(B) Based on the number of iterations represented by $q$, the gradient directions of the residuals were calculated using Eq. (7).

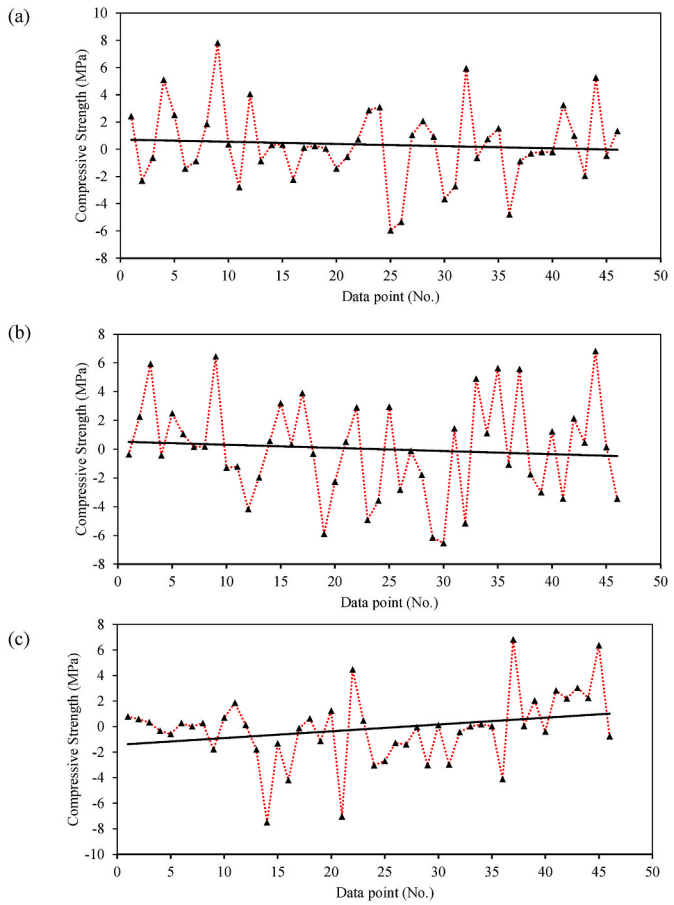


**Fig. 8.** Error analysis (a) ANN (b) GEP (c) GBT

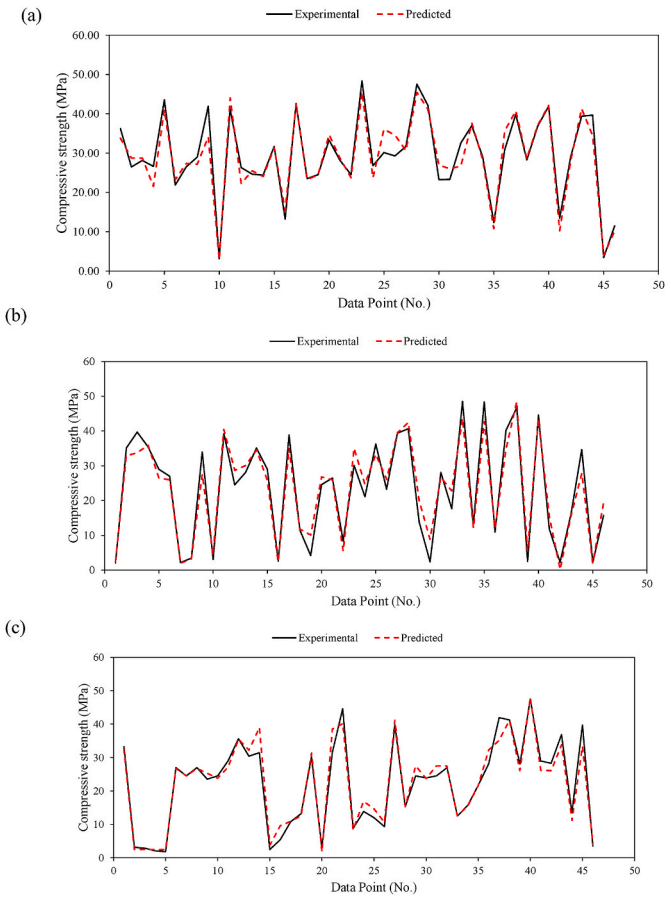


**Fig. 9.** Tracing of experimental results by the predictions (a) ANN (b) GEP (c) GBT.

$$y_i^* = -\left[\frac{\partial L(y_i, F(x_i))}{\partial F(x_i)}\right]_{F(x)=F_{q-1(x)}}, i = \{1, 2, \ldots, M\} \quad \text{Eq. 7}$$

(C) A subset of the dataset was fitted by using a basic classifier to obtain the initial model. The parameter $a_q$ of the model, $h(x_i; a_q)$ is determined for the model to be fitted (Eq. (8)).

$$a_q = \arg\min_{\alpha,\gamma} \sum_{i=1}^{N} \left[y_i^* - \alpha h(x_i; a)\right]^2 \quad \text{Eq. 8}$$

(D) After minimizing the loss function, the current weight of the model was computed using Eq. (9).

$$\alpha_m = \arg\min_{\alpha,\gamma} \sum_{i=1}^{N} L\left(y_i, F_{q-1}(x) + \alpha h(x_i; a)\right) \quad \text{Eq. 9}$$

(E) With the conclusion of step (D), the model is updated and represented by Eq. (10).

$$F_q(x) = F_{q-1}(x) + \alpha_m h(x_i; a) \quad \text{Eq. 10}$$

### 2.3.2. Gene expression programming (GEP)

Gene expression programming (GEP) is a versatile and soft computing technique that incorporates both gene algorithms and genetic programming and has been utilized by many researchers in different engineering applications. GEP has been deployed in myriad engineering applications to develop empirical equations for estimating different concrete properties developed from different materials. Genetic programming (GP) is a valuable and powerful soft computing method that ignores previous forms of existing relationships for model development [95,96]. GEP is an extension of GP and is a recent introduction that encodes samples or small-sized programs and utilizes them for fixed-length linear chromosomes. Ferreira proposed the GEP technique as a modification of the GP methodology to overcome its discrepancies [97]. The significant alteration was that only the genome is transmitted subsequently to another generation and that single chromosomes can establish entities that are composed of genes divided into head and tail parts [98]. These entities are known as expression trees (ET). GEPs are inspired by the reproduction of DNA molecules at the genetic level [99]. The computational time of GEP depends on the number of available chromosomes, which in turn controls the magnitude of the population. Genetic operators aid the genetic diversity of chromosomes. The chromosome that produces the greatest outcomes is passed down to the succeeding generations, and the process continues until an acceptable fitness level is achieved [100]. Within GEP, every gene is represented by fitting the length parameters, terminal sets of constants, and arithmetic operations as functions. Additionally, both the related function and chromosomal symbol have a stable connection with genetic code operators. The data required for the construction of an empirical model are encoded in the chromosomes, and a novel software called Karva was created to infer these data [100].

### 2.3.3. Artificial neural network (ANN)

Artificial neural networks (ANNs) are algorithms that mimic the internal framework (neurons) of a biological nervous system, similar to the connection between neurons in the human brain [101–104]. Similar to other ML algorithms, ANN is a computational and mathematical technique employed to simulate the interdependencies between the input parameters and output variable(s) [102]. The most used type of

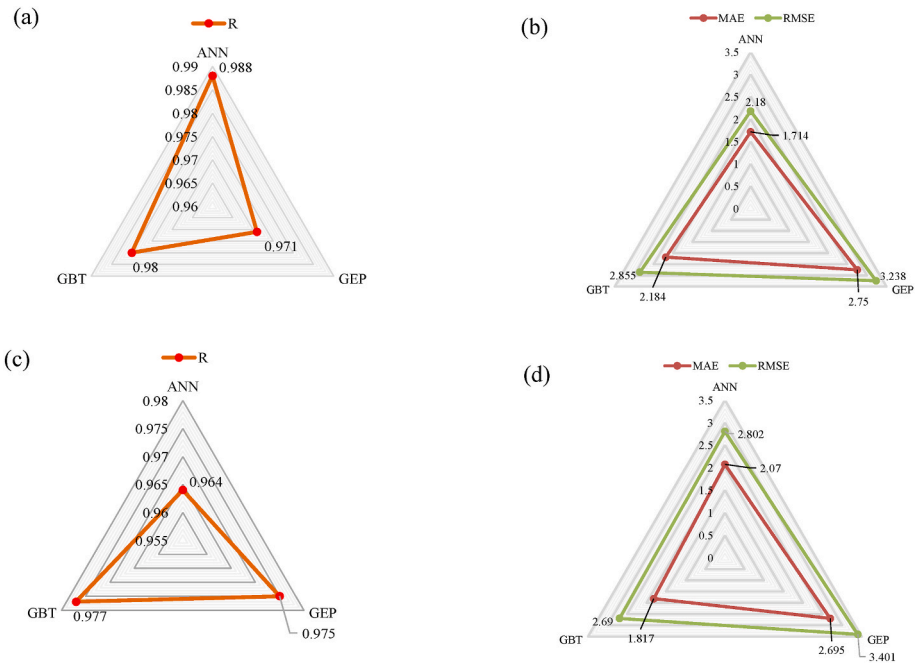


**Fig. 10.** Comparison of the developed AI models (a,b) for training and (c,d) for validation data.

**Table 7**
Predicted/experimental results for the developed models.

| Predicted/experimental | ANN Model | | GEP Model | | GBT Model | |
|---|---|---|---|---|---|---|
| | Frequency | Cumulative | Frequency | Cumulative | Frequency | Cumulative |
| 0.5 | 0 | 0.00% | 1 | 2.17% | 0 | 0.00% |
| 0.7 | 0 | 0.00% | 1 | 4.35% | 1 | 2.17% |
| 0.8 | 1 | 2.17% | 0 | 4.35% | 0 | 2.17% |
| 0.85 | 4 | 10.87% | 2 | 8.70% | 4 | 10.87% |
| 0.9 | 5 | 21.74% | 7 | 23.91% | 2 | 15.22% |
| 0.95 | 4 | 30.43% | 8 | 41.30% | 6 | 28.26% |
| 1 | 11 | 54.35% | 5 | 52.17% | 12 | 54.35% |
| 1.05 | 11 | 78.26% | 6 | 65.22% | 6 | 67.39% |
| 1.1 | 3 | 84.78% | 3 | 71.74% | 2 | 71.74% |
| 1.15 | 2 | 89.13% | 1 | 73.91% | 4 | 80.43% |
| 1.2 | 5 | 100.00% | 4 | 82.61% | 1 | 82.61% |
| 1.5 | 0 | 100.00% | 5 | 93.48% | 6 | 95.65% |
| More | 0 | 100.00% | 3 | 100.00% | 2 | 100.00% |

**Table 8**
Simulated dataset for parametric ad sensitivity Analysis.

| Variable input parameters | | No. of datapoints | Constant input parameters |
|---|---|---|---|
| Parameter | Range | | |
| Density | 430–2065 | 10 | w/c = 0.41, s/c = 1.04 |
| w/c | 0.26–0.83 | 10 | Density = 1542; s/c = 1.04 |
| s/c | 0–4.293 | 10 | Density = 1542; w/c = 0.41 |

neural network is the feedforward neural network, and the most commonly used type is the multilayer perceptron (MLP), which consists of an input layer, one or more hidden layers, and output layer (s). Although the number of neurons deployed in each layer depends on many parameters, there is no connection between the neurons present in each layer. The number of input and output neurons required for modelling depends on the input and output variables. The hidden layer is where computation takes place, and the number of neurons in this layer varies, the number of which needs to be determined for the appropriate response to be reached [105]. To train the neural network, data are introduced into the input and output layers, and appropriate models are created. The weights and biases of the network were adjusted to achieve the minimum error by calculating the difference between the output predicted values and actual values [106]. In most situations, an ANN is an adaptive system that can update its model in response to the relevant information flowing through the network during the learning phase. An ANN can be used to represent almost any complicated relationship between the inputs and outputs in the data [107].

### 2.4. Prediction modelling

As stated earlier, three AI methods were employed to predict the compressive strength of the lightweight foamed concrete. Eighty percent of the data was used to train the ANN model with the Levenberg-Marquardt backpropagation algorithm owing to its high accuracy and fast convergence behavior [108]. Several trials were performed using one, two, and three hidden layers and several neurons. Optimum results were obtained using a single hidden layer with 10 neurons, as shown in Table 3. The data division was kept random between training and validation. The correlation coefficient, R (Eq. (11)) was used to assess the predicted yield. The architecture of the developed ANN model is presented in Fig. 3, which shows that three inputs, presented in the form

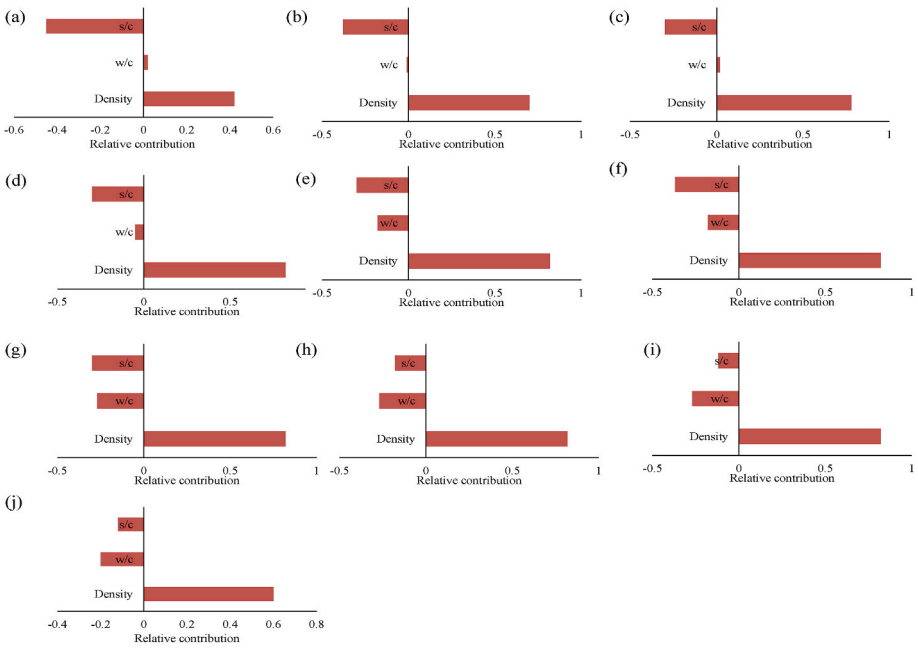


**Fig. 11.** Relative contribution of variable density for constant average w/c ratio of 0.416 and s/c of 1.04; density equalling 430, 593, 756, 919, 1082, 1245, 1408, 1571, 1734, and 2065 from a to j, respectively.

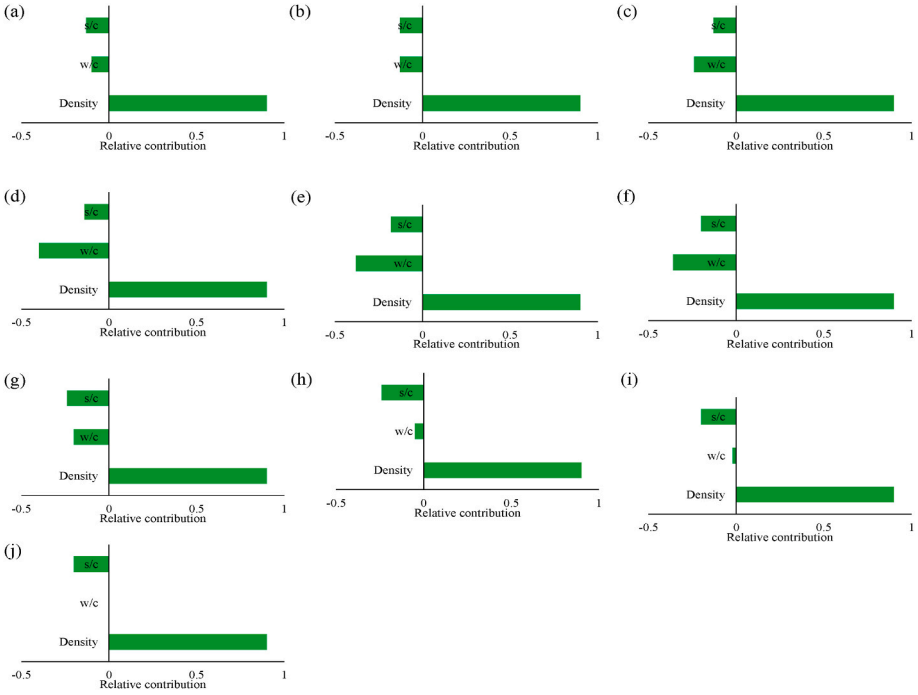


**Fig. 12.** Relative contribution of variable w/c ratio for constant average density of 1542 kg/m$^3$ and s/c of 1.04; w/c equalling 0.26, 0.28, 0.30, 0.35, 0.40, 0.45, 0.50, 0.60, 0.70, and 0.83 from a-j, respectively.

of three neurons, were used to estimate the compressive strength with a single hidden layer of neurons.

The GEP algorithm has the valuable feature of creating a simple mathematical model by deploying a given number of input variables to estimate a target variable [109]. This study also aimed to develop a mathematical model that can correlate the compressive strength of foam concrete with input attributes. A flow diagram depicting optimal model development is shown in Fig. 4. The input data were partitioned into 80% training data and 20% validation data. The hyperparameter of the better GEP model is the trial-and-access method in terms of using variable setting parameters, that is, the number of genes, chromosomes and head size [110–115]. The setting parameters were changed according to the flowchart (Fig. 4) and Table 5, employing the root mean square error (RMSE) as a fitness function. In addition, the models were assessed using R, the mean absolute error (MAE) and the relative squared error (RSE), whose mathematical equations are expressed in Eqs. (11) to Eq. (14). Five models were created, as listed in Table 4. All the developed models of GEP reflected a close agreement with the experimental values, yielding R significantly higher than 0.9 for both the training and validation data. However, the model developed using 200

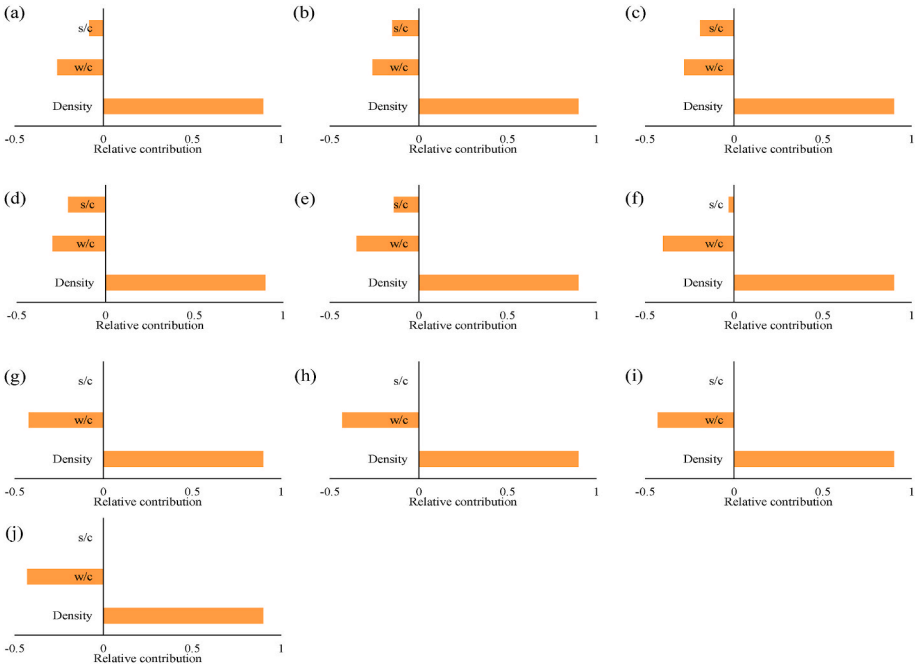


**Fig. 13.** Relative contribution of variable s/c ratio for constant average density of 1542 kg/m3 and w/c of 0.41; s/c equalling 0, 0.3, 0.50, 1.0, 1.40, 2.0, 2.5, 3.0, 3.5, and 4.29 from a-j, respectively.

chromosomes with 12 head sizes and five genes had the highest correlation and lowest values of MAE, RMSE and RSE in both the training and validation phases. Hence, this model, represented as GEP4, was used to create a mathematical equation based on the expression trees (Fig. 6) and the MATLAB model derived from the modelling process. As shown in Table 5, +,-,*,/,x^(1/3),x^2 were used as function sets for generating expression trees and addition was used as a function for linking expression trees. It was also observed that complexifying the function set increased the robustness of the model; however, this made the output equation complex. Therefore, a simple function set was fed into the model.

$$R = \frac{\sum_{i=1}^{n}(e_i - \overline{e}_i)(m_i - \overline{m}_i)}{\sqrt{\sum_{i=1}^{n}(e_i - \overline{e}_i)^2 (m_i - \overline{m}_i)^2}} \quad \text{Eq. 11}$$

$$MAE = \frac{\sum_{i=1}^{n}|e_i - m_i|}{n} \quad \text{Eq. 12}$$

$$RMSE = \sqrt{\frac{\sum_{i=1}^{n}(e_i - m_i)^2}{n}} \quad \text{Eq. 13}$$

$$RSE = \frac{\sum_{i=1}^{n}(e_i - m_i)^2}{\sum_{i=1}^{n}(\overline{e} - m_i)^2} \quad \text{Eq. 14}$$

where $e_i$ and $m_i$ are the nth experimental and model CS (MPa), respectively, $\overline{e_i}$ and $\overline{m_i}$ denote the average values of the experimental and model CS (MPa), respectively, and n is the number of samples in the dataset, where n denotes the total number of sample points.

The GBT model was generated in the RapidMiner environment. The data was loaded into the RapidMiner environment using *retrieve data* operator. The data was then given the target and contributing attributes using *select attribute* operator. With the *split data* operator, the data was randomly divided into training and validation data employing. Overall, the modelling involves basic data processing, feature selection as discussed above, followed by optimization of GBT model (using grid search for number of trees, maximal depth and learning rate). The optimized model was subsequently used for the validation of the model (Fig. 5). The methodology used in the current study was in accordance with those adopted by Amin et al. [78] and Iqbal et al. [81]. The hyperparameters of the GBT model were optimized. The initial values of the GBT hyper-parameters, that is, the number of trees, maximal depth, and learning rate, were randomly initiated with lower bounds of 30, 2, and 0.001, respectively. The optimum performance for the developed model was achieved for the number of trees, maximal depth and learning rate of 90, 7, and 0.10, respectively, as shown in Table 6.

## 3. Results and discussions

### 3.1. Predictive performance and validation

#### 3.1.1. ANN

A graphical demonstration of the experimental versus predicted values of the compressive strength using the proposed ANN-based model is shown in Fig. 7. The closer the points are to the regression line (1:1 plot), the better is the efficacy of the formulated AI model [116]. The ANN model precisely captures the impact of the input parameters on predicting the compressive strength. The correlation coefficients for the training and validation datasets are 0.988 and 0.960, respectively, suggesting a strong correlation between the experimental and predicted results [117]. However, it was also found that R is insensitive to the multiplication and division of the compressive strength [118]; therefore, the RMSE and MAE indices were evaluated to better judge the performance of the model. Additionally, it is also confirmed from the substantially decreased values of these performance indices (i.e., $RMSE_{training} = 2.18$, $RMSE_{validation} = 2.80$, $MAE_{training} = 1.71$, $MAE_{validation} = 2.07$). In addition, the error analysis plot in Fig. 8 shows that the compressive strength errors range from zero to 1.4 MPa. Finally, the tracing of experimental and ANN-modelled compression strength values in Fig. 9a show larger deviations mainly in two regions, that is, data points from 0 to 8 and 25 to 32.

#### 3.1.2. GEP

According to Ferreira [111], the language of genes and expression trees (ETs) are interrelated, and knowledge of one helps understand the other. To determine the simple empirical relationships for calculating

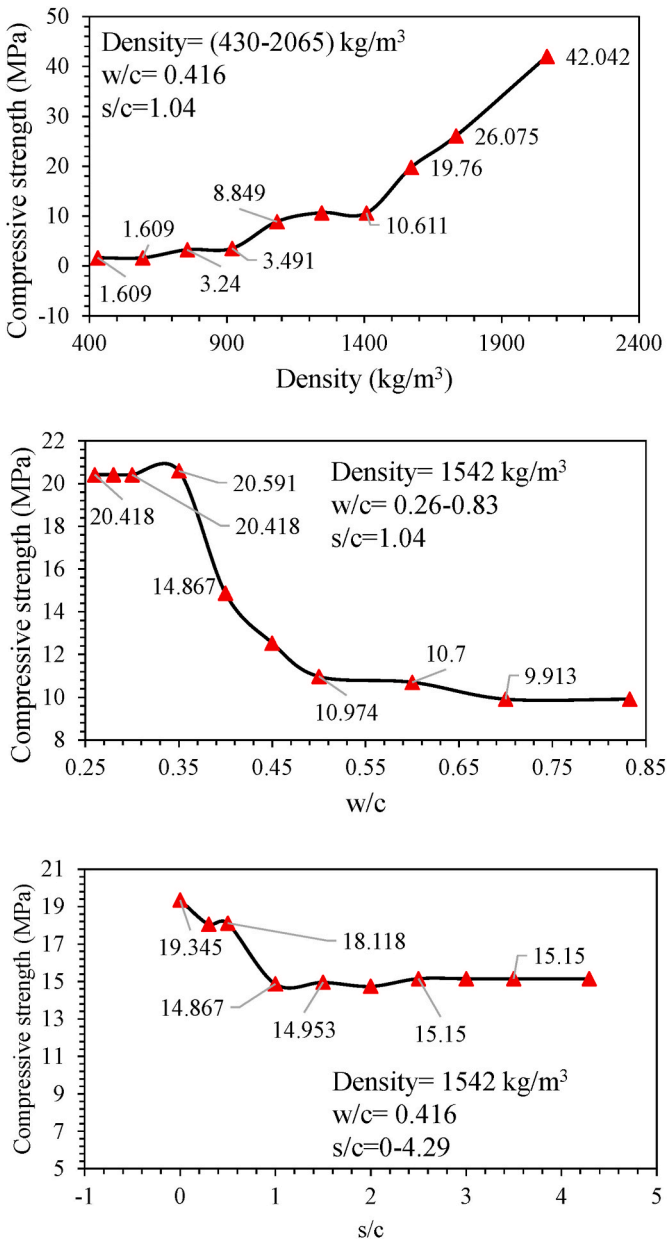


**Fig. 14.** Parametric analysis of each input parameter.

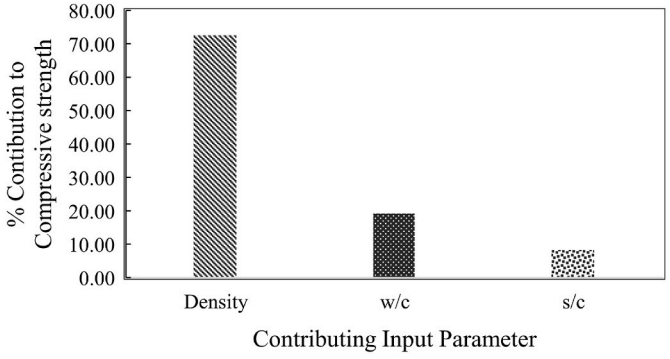


**Fig. 15.** Relative contribution (%) of input variables in yielding compressive strength.

the compressive strength, Fig. 6 illustrates typical ETs for the GEP algorithm of the formulated models. The sub-ETs (1–3) of the compressive strength of concrete exhibit six fundamental mathematical functions: +, −, x, ÷, 3Rt and $x^2$. The mechanism of these sub-ETs consists of the regulation of their maximum width and depth ($w_{max}$ and $d_{max}$, respectively) by the head size ($h_s$), which can be determined from Eq. (15) and Eq. (16).

$$w_{max} = [(a_{max} - 1) * h_s] + 1 \quad \text{Eq. 15}$$

$$d_{max} = \left(\frac{h_s + 1}{a_{min}}\right) * \left(\frac{a_{min}}{2}\right) \quad \text{Eq. 16}$$

such that $a_{min}$ represents the minimum arity (i.e., the lowest possible arguments of the functions), whereas $a_{max}$ represents the maximum arity (i.e., the largest possible arguments of the functions). In this study, $a_{min}$ was considered to be zero, whereas $a_{max}$ was considered to be two for all formulated AI models.

After the formulation of the GEP model, the ETs were decoded to derive a simple mathematical expression for compressive strength as a function of the selected input parameters. In accordance with the hyperparameter settings for the GEP model, the Karva notation or K-expression [119] was first changed into ETs that were subjected to decoding to achieve an easy-to-use mathematical equation in the form of Eq. (17), below:

$$\acute{f}_c = A + B + C + D + E \quad \text{Eq. 17}$$

A = ((gep3Rt (−5.13) +(((w/c)-1.90) *((s/c) +8.32)) *((w/c)/((0.64-(w/c)) +((w/c) ^2)))).
B = gep3Rt(((((((s/c) +(w/c)) +(s/c)) -((w/c) +1.83)) *(((w/c)/8.16) +gep3Rt((s/c)))) ^2)-9.49)).
C = (gep3Rt(((-1818.71/(w/c)) +(15.38^2)) +((s/c) -(D))) +(D/(((w/c) +3.99) *((s/c) +7.48))])
D = (gep3Rt(gep3Rt((D*(((9.25^2) *(9.25 + 7.52)) -((-6.22-3.52) +D))))) ^2).
E = (4.25*(-5.46/(((s/c)/(((s/c) +(w/c)) ^2)) +(((w/c) -(s/c)) +(-1.49/8.34))).
Where D = density in kg/m$^3$, w/c = water-cement ratio in g/g, s/c = sand-cement ratio in g/g, gep3Rt = $\sqrt[3]{()}$

These equations can be used directly to estimate the compressive strength of concrete [120,121]. A graphical demonstration of the experimental versus predicted values of compressive strength using the proposed GEP-formulated model is shown in Fig. 7. It is pertinent to mention that the results of the validation dataset were better than those of the training datasets, unlike those of the two other AI methods deployed here. A strong correlation exists between the input variables at higher R values [118,122]. Regarding the accuracy of the GEP model, it was observed that the difference in all the considered performance indices (R, RMSE, and MAE) in the training and validation datasets was minimal, that is, 0.004, 0.17, and 0.055, respectively. This shows that the concentration of the error scatter is approximately zero. Moreover, the error analysis graph in Fig. 8 depicts that the compressive strength exhibits errors between 0.3 and −0.3 MPa, which represents the superior performance of the developed GEP model. Finally, the tracing of the experimental and GEP-modelled output values in Fig. 9 reveals a lesser deviation among the values; however, a slight deviation was observed in the case of datapoints 0–5, 10–15, and 24–30.

### 3.1.3. GBT

A graphical demonstration of the experimental and predicted values of compressive strength using the proposed GBT prediction model is shown in Fig. 7c, where all three values of the performance indices outperform those of the ANN and GEP models. It can be seen that the training and validation datasets exhibit almost identical R values, i.e., 0.980 and 0.977, respectively. The difference was larger in the MAE

values (2.184 and 1.817) in contrast to the RMSE values of 2.8555 and 2.690 for the training and validation sets, respectively. Similarly, the error analysis plot in Fig. 8c reveals that the compressive strength has errors in the range of unity to −1.7 MPa. Eventually, the tracing of experimental and GBT modelled values can be seen in Fig. 9c, where the variations in both values are dispersed, unlike the ANN and GEP approaches, and can therefore be recorded for six small ranges of the data points, including 7–13, 15–17, 23–25, 28–32, 36–38, and 41–44.

### 3.2. Comparison of the models

Fig. 10 shows a comparison of the developed models in the form of a radar plot. A radar plot conveys information more clearly than other charts, particularly for a larger volume of data [123]. Each model investigated in this study was represented by a spoke projected from the central point. Typically, the radar plot adopts a circular arrangement. Three AI models were investigated; they formed a triangular arrangement. Smaller triangles represent the scale of each series. The gap between the two triangles in the case of R was 0.05, whereas, in the case of MAE and RMSE, it was 0.5. Several researchers have used radar plots in various fields to obtain multivariate data [124,125].

When comparing the correlation between the observed and predicted results, the GBT model performed better in the validation phase, with R = 0.977. The GBT model also showed close agreement during training, with an R-value of 0.98. Comparable correlation results were obtained for the ANN and GEP models; however, the ANN model was slightly overfitted during training, resulting in a reduced correlation compared to the training model. Overfitting was not observed in the GEP model (Fig. 10a and c). An error comparison of the models can be seen in Figs. 10b and 9d. The lowest MAE and RMSE for the validation data were 1.817 MPa and 2.69 MPa, for the GBT model. The ANN model followed the GBT model in terms of accuracy, whereas the GEP model ranked third while investigating the accuracy. The comparison of the developed models was supplemented with the predicted-experimental ratios (Table 7). In this comparison, 100% of the validation records for ANN models are within ±20%, whereas, for the GEP and GBT models, the percentage of data points with 20-% is 78.26 and 80.4%, respectively. Herein, the ANN model excels GBT model; however, due to other good performance regarding statistical indices, the GBT model has been used for parametric analysis.

The performance of GBT model was also compared with other studies conducted by past researchers. Dao et al. [77] evaluated the compressive strength of FC using conventional ANN on the basis of 220 experimental results from the literature. A comparable performance was obtained; however, the optimization of w/c ratio and s/c ratio were not investigated. Ly et al. [18] achieved maximum value of R equalling 0.959 while investigating ANN model on 375 data points. The effect of each input parameter was studied in the form of partial dependence plots, figuring out the increasing or decreasing trend of compressive strength with change input variable; however, the optimized combined effect of input variables was not reported. The study conducted herein describes the detailed contribution of each variable at various stages of density, w/c ratio and s/c ratio.

### 3.3. Parametric and sensitivity analysis

Owing to the robustness of the GBT model, parametric and sensitivity analyses were conducted on the simulated dataset (Table 8). Simulated data were generated such that one input parameter was changed between its extremes, whereas the other variables were maintained at their average values, as shown in Table 8. Fig. 11 to Fig. 13 show the stepwise variation in the relative contribution of the input variables and the change in compressive strength with an increase in the density of foam concrete. At a fixed w/c ratio of 0.416 and s/c ratio of 1.04, the compressive strength increased almost linearly with rise in density, as shown in Fig. 14. Fig. 11 illustrates that the relative contribution of density increased with increasing density. The s/c ratio of 1.04 negatively contributed to the compressive strength and was comparatively more negative in low-density concrete than in high-density concrete. A w/c ratio of 0.41 contributed negligibly at the initial stage of increasing the density, whereas it negatively contributed to the compressive strength at a high density of concrete. An increase in the w/c up to 0.35 ratio initially increased the compressive strength. Further increase in the w/c ratio drastically decreased the compressive strength, as shown in Fig. 14. Fig. 12 also shows the negative impact of increasing the w/c. An increase in w/c beyond 0.6 reflected no contribution to the compressive strength. An increase in s/c also negatively affected the compressive strength of the foamed concrete, as supported by Figs. 13 and 14. The sensitivity analysis illustrated in Fig. 15 shows that density is the most influential factor in the compressive strength of concrete, followed by the w/c and s/c ratios.

## 4. Concluding remarks

This research presents the findings of three prediction models, ANN, GEP and GBT models that are capable of estimating the compressive strength of foamed concrete (FC). Most empirical models for predicting the compressive strength of FC are calibrated using experimental data, which are limited by the number of input parameters used in the equations, thus making their predictions mostly extrapolative. Again, prediction with an empirical model requires empirical constants that are difficult to obtain when describing the complex relationship between mixture proportions and compressive strength. This study focused on the optimization of input variables on the basis of a more robust prediction model among the three AI models. Following conclusions were drawn from this study.

Pearson's correlation coefficients indicated a strong positive correlation between the density of the FC and compressive strength. The water-cement ratio interpreted a strong negative correlation, whereas send to cement ratio also showed a moderate negative correlation to the compressive strength of FC. The results of a Pearson's correlations were also supported by parametric and sensitivity analyses performed based on a highly accurate AI model. While optimizing the developed model, the optimum results of the ANN models were achieved by employing the Levenberg–Marquardt algorithm with one hidden layer and 10 neurons. The data trained using the GEP algorithm were assessed in several trials by changing the number of chromosomes, the head size and the number of genes. The best hyperparameters, namely, the number of chromosomes, head size and number of genes for GEP, were 200, 12, and 5, respectively. Ninety (90) trees with seven (7) maximal depths and a learning rate of 0.10 provided the best GBT model.

When assessing the performance of the AI models, all the models yielded a correlation of R significantly higher than 0.8, ranging from 0.971 to 0.988 for the training and 0.96 to 0.977 for the validation data, reflecting a close agreement between the experimental and predicted results. The highest correlation (0.977) in the validation data was obtained for the GBT model, and the lowest MAE and RMSE (2.184 and 2.85, respectively) for the validation data were obtained for the GBT model. Hence, the GBT model surpassed the other models in terms of accuracy, followed by the ANN and GEP models, respectively. However, the significance of the GBT model cannot be neglected because it expresses the target variable as a simple mathematical relationship. During the variation in the quantity of water in parametric analysis, maximum concrete strength was achieved at w/c ratio range of 0.35 to 0.40 at an average value of density and s/c ratio. Exceeding s/c from 0.4 leads to a considerable reduction in the compressive strength. Parametric and sensitivity analyses revealed that the density of the concrete play a vital role in contributing to the compressive strength of the FC, followed by the w/c and s/c ratios. The current models employed three inputs for predicting the compressive strength of FC on the basis of 232 experimental records collected from the literature. The authors opine that new prediction models shall be developed based on a wide range of

experimental work obtained from a single source. Besides, the role of variable dosage of the foaming agent shall also be investigated in the future using AI modelling.

## Authors contribution

**Conceptualization**: Babatunde Abiodun salami, Mudassir Iqbal, Fazal E. Jalal, Abdulazeez Abdulraheem; **Methodology**: Fazal E. Jalal, Mudassir Iqbal, Abidhan Bardhan, Arshad Jamal; **Data Collection**: Wasiu Alimi, T. Tafsirojjaman, Mudassir Iqbal, Babatunde Abiodun Salami; **Writing Original Draft**: Fazal E. Jalal, Babatunde Abiodun salami, Mudassir Iqbal, Arshad Jamal, Abidhan Bardhan, Yue Liu; **Reviewing:** Mudassir Iqbal, Fazal E. Jalal, T. Tafsirojjaman, Yue Liu**;** Funding **Acquisition**: Yue Liu, T. Tafsirojjaman.

## Declaration of competing interest

The authors declare that they have no known competing financial interests or personal relationships that could influence the work reported in this study.

## Data availability

Data will be made available on request.

## Acknowledgement

The authors would like to acknowledge the funding provided by International Research Cooperation Seed Fund of Beijing University of Technology (2021B11). Moreover, the authors also acknowledge the literature resources of Shanghai Jiao Tong University, China; King Fahd University of Petroleum and Minerals, Saudi Arabia; the University of Engineering and Technology, Peshawar, Pakistan; and Khushal Khan Khattak University, Karak, Pakistan.

## Appendix A. Supplementary data

Supplementary data to this article can be found online at https://doi.org/10.1016/j.cemconcomp.2022.104721.

## References

[1] M. Shariati, D.J. Armaghani, M. Khandelwal, J. Zhou, M. Khorami, Assessment of longstanding effects of fly ash and silica fume on the compressive strength of concrete using extreme learning machine and artificial neural network, J. Adv. Eng. Computation 5 (2021) 50–74, https://doi.org/10.25073/JAEC.202151.308.

[2] M. Shariati, M.S. Mafipour, B. Ghahremani, F. Azarhomayun, M. Ahmadi, N. T. Trung, A. Shariati, A novel hybrid extreme learning machine–grey wolf optimizer (ELM-GWO) model to predict compressive strength of concrete with partial replacements for cement, Eng. Comput. 38 (2022) 757–779, https://doi.org/10.1007/S00366-020-01081-0/TABLES/7.

[3] M. Amran, Y.H. Lee, N. Vatin, R. Fediuk, S. Poi-Ngian, Y.Y. Lee, G. Murali, Design efficiency, characteristics, and utilization of reinforced foamed concrete: a review, Crystals 10 (2020) 948, https://doi.org/10.3390/CRYST10100948, 10 (2020) 948.

[4] Y.H.M. Amran, N. Farzadnia, A.A.A. Ali, Properties and applications of foamed concrete; a review, Construct. Build. Mater. 101 (2015) 990–1005, https://doi.org/10.1016/J.CONBUILDMAT.2015.10.112.

[5] D. Falliano, D. de Domenico, G. Ricciardi, E. Gugliandolo, Experimental investigation on the compressive strength of foamed concrete: effect of curing conditions, cement type, foaming agent and dry density, Construct. Build. Mater. 165 (2018) 735–749, https://doi.org/10.1016/J.CONBUILDMAT.2017.12.241.

[6] D. Niu, L. Zhang, Q. Fu, B. Wen, D. Luo, Critical conditions and life prediction of reinforcement corrosion in coral aggregate concrete, Construct. Build. Mater. 238 (2020), 117685, https://doi.org/10.1016/J.CONBUILDMAT.2019.117685.

[7] X. Tan, W. Chen, J. Wang, D. Yang, X. Qi, Y. Ma, X. Wang, S. Ma, C. Li, Influence of high temperature on the residual physical and mechanical properties of foamed concrete, Construct. Build. Mater. 135 (2017) 203–211, https://doi.org/10.1016/J.CONBUILDMAT.2016.12.223.

[8] Ş. Kilincarslan, M. Davraz, M. Akça, The effect of pumice as aggregate on the mechanical and thermal properties of foam concrete, Arabian J. Geosci. 11 (2018) 1–6, https://doi.org/10.1007/S12517-018-3627-Y, 11. 11 (2018.

[9] R.K. Dhir, M.D. Newlands, Aikaterini McCarthy, INTRODUCTION TO FOAMED CONCRETE: WHAT, WHY, HOW?, 2005, p. 158, https://doi.org/10.1680/UOFCIC.34068.0001.

[10] A. Hajimohammadi, T. Ngo, P. Mendis, T. Nguyen, A. Kashani, J.S.J. van Deventer, Pore characteristics in one-part mix geopolymers foamed by H2O2: the impact of mix design, Mater. Des. 130 (2017) 381–391, https://doi.org/10.1016/J.MATDES.2017.05.084.

[11] A.A. Sayadi, J.v. Tapia, T.R. Neitzert, G.C. Clifton, Effects of expanded polystyrene (EPS) particles on fire resistance, thermal conductivity and compressive strength of foamed concrete, Construct. Build. Mater. 112 (2016) 716–724, https://doi.org/10.1016/J.CONBUILDMAT.2016.02.218.

[12] S. Sidhardhan, A. Sagaya Albert, Experimental investigation on light weight cellular concrete by using glass and plastic waste–a review, Int. J. Sci. Technol. Res. 9 (2020) 1947–1952.

[13] A.M. Hameed, R.F. Hamada, Using the glass and rubber waste as sustainable materials to prepare foamed concrete with improved properties, in: IOP Conference Series: Materials Science and Engineering, 2020, https://doi.org/10.1088/1757-899X/881/1/012188.

[14] H.Y. Tiong, S.K. Lim, Y.L. Lee, C.F. Ong, M.K. Yew, Environmental impact and quality assessment of using eggshell powder incorporated in lightweight foamed concrete, Construct. Build. Mater. 244 (2020), https://doi.org/10.1016/j.conbuildmat.2020.118341.

[15] L.S. Kang, F.K. Poh, L.F. Wei, T.H. Yong, L.Y. Ling, L.J. Hock, K.Y. Jin, Acoustic properties of lightweight foamed concrete with eggshell waste as partial cement replacement material, Sains Malays. 50 (2021) 537–547, https://doi.org/10.17576/jsm-2021-5002-24.

[16] A.A. Jhatial, W.I. Goh, N. Mohamad, K.H. Mo, A. Mehroz, Thermomechanical evaluation of sustainable foamed concrete incorporating palm oil fuel ash and eggshell powder, J. Eng. Res. (Kuwait) 9 (2021) 64–79, https://doi.org/10.36909/jer.v9i3A.8290.

[17] M.F. Omar, M.A.H. Abdullah, N.A. Rashid, A.L.A. Rani, Partially replacement of cement by sawdust and fly ash in lightweight foam concrete, IOP Conf. Ser. Mater. Sci. Eng. 743 (2020), 012035, https://doi.org/10.1088/1757-899X/743/1/012035.

[18] H.-B. Ly, M.H. Nguyen, B.T. Pham, Metaheuristic optimization of Levenberg–Marquardt-based artificial neural network using particle swarm optimization for prediction of foamed concrete compressive strength, Neural Comput. Appl. 33 (2021) 17331–17351, https://doi.org/10.1007/S00521-021-06321-Y, 24. 33 (2021).

[19] D. Falliano, D. de Domenico, G. Ricciardi, E. Gugliandolo, Key factors affecting the compressive strength of foamed concrete, IOP Conf. Ser. Mater. Sci. Eng. 431 (2018), 062009, https://doi.org/10.1088/1757-899X/431/6/062009.

[20] A.M. Neville, Properties of Concrete, 2011.

[21] M.R. Jones, Foamed concrete for structural use, in: Proceedings of One Day Seminar on Foamed Concrete: Properties, Applications and Latest Technological Development, 2001, pp. 27–60.

[22] R. Othman, R.P. Jaya, K. Muthusamy, M. Sulaiman, Y. Duraisamy, M.M.A. B. Abdullah, A. Przybył, W. Sochacki, T. Skrzypczak, P. Vizureanu, A.V. Sandu, Relation between density and compressive strength of foamed concrete, Materials 14 (2021) 2967, https://doi.org/10.3390/MA14112967.

[23] C. Bing, W. Zhen, L.N.-J. of materials in civil engineering, undefined 2012, Experimental research on properties of high-strength foamed concrete, Ascelibrary.Org. 24 (2012) 113–118, https://doi.org/10.1061/(ASCE)MT.1943-5533.0000353.

[24] L. de Rose, J. Morris, The Influence of Mix Design on the Properties of Microcellular Concrete, 1999. https://books.google.com/books?hl=en&lr=&id=e7pFNxU_OKkC&oi=fnd&pg=PA185&ots=DrkiqCyiu7&sig=m0ehQy1WTbex5ydtMm_X9ESmdBo. (Accessed 5 November 2021).

[25] K.C. Brady, R.A. Watts, I.R. Jones, Specification for Foamed Concrete, 2001.

[26] Y.H.M. Amran, N. Farzadnia, A.A.A. Ali, Properties and applications of foamed concrete; a review, Construct. Build. Mater. 101 (2015) 990–1005, https://doi.org/10.1016/J.CONBUILDMAT.2015.10.112.

[27] A. Raj, D. Sathyan, K.M. Mini, Physical and functional characteristics of foam concrete: a review, Construct. Build. Mater. 221 (2019) 787–799, https://doi.org/10.1016/J.CONBUILDMAT.2019.06.052.

[28] J. Zhang, J. Li, L. Zhang, Z. Liu, Z. Jiang, Dynamic performance of foam concrete with recycled coir fiber, Frontiers Mater. 7 (2020) 320, https://doi.org/10.3389/FMATS.2020.567655/BIBTEX.

[29] Y.H. Mugahed Amran, R. Alyousef, H. Alabduljabbar, M.H.R. Khudhair, F. Hejazi, A. Alaskar, F. Alrshoudi, A. Siddika, Performance properties of structural fibred-foamed concrete, Results Eng. 5 (2020), https://doi.org/10.1016/j.rineng.2019.100092.

[30] K. Ramamurthy, E. Nambiar, G.R. C, concrete, undefined, A Classification of Studies on Properties of Foam Concrete, Elsevier, 2009 (n.d. https://www.sciencedirect.com/science/article/pii/S0958946509000638. (Accessed 5 November 2021).

[31] A. Just, B.M.-M. characterization, undefined, Microstructure of High-Strength Foam Concrete, Elsevier, 2009 (n.d.), https://www.sciencedirect.com/science/article/pii/S1044580308003392. (Accessed 5 November 2021).

[32] N. Uddin, F. Fouad, U.K. Vaidya, A. Khotpal, J.C. Serrano-Perez, Structural characterization of hybrid fiber reinforced polymer (FRP)-Autoclave aerated concrete (AAC) panels, Http://Dx.Doi.Org/10.1177/0731684406065090. 25, https://doi.org/10.1177/0731684406065090, 2016, 981-999.

[33] S. Mindess, Developments in the formulation and reinforcement of concrete (accessed November 5, 2021), https://books.google.com/books?hl=en&lr=&id=YGGdDwAAQBAJ&oi=fnd&pg=PP1&dq=S.+Mindess+,+Developments

+in+the+Formulation+and+Reinforcement+of+Concrete,+Wood+head+Publishing+and+Maney+Publishing,+Institute+of+Materials,+Minerals++Mining+CRC+press+Boca+Raton+Boston+New+York+Washington,+DC,+Elsevier,+2014.&ots=1dYAFvb9oy&sig=TMT40zAIt0rKAc8fJ9IZFflxFdQ, 2019.
[34] P. Tikalsky, J. Pospisil, W.M. C, concrete research, undefined, A Method for Assessment of the Freeze–Thaw Resistance of Preformed Foam Cellular Concrete, Elsevier, 2004 (n.d.), https://www.sciencedirect.com/science/article/pii/S0008884603003909. (Accessed 5 November 2021).
[35] M. Jones, A.M. the international conference held at, undefined 2005, Behaviour and assessment of foamed concrete for construction applications, Icevirtuallibrary.Com (n.d.), https://www.icevirtuallibrary.com/doi/abs/10.1680/uofcic.34068.0008. (Accessed 5 November 2021).
[36] H. Weigler, S.K.-I.J. of C.C. and, undefined, Structural Lightweight Aggregate Concrete with Reduced Density—Lightweight Aggregate Foamed Concrete, Elsevier, 1980 (n.d.), https://www.sciencedirect.com/science/article/pii/0262507580900299. (Accessed 5 November 2021).
[37] K. Yang, K. Lee, J. Song, M.G.-J. of C. Production, undefined, Properties and Sustainability of Alkali-Activated Slag Foamed Concrete, Elsevier, 2014 (n.d.), https://www.sciencedirect.com/science/article/pii/S0959652613009220. (Accessed 5 November 2021).
[38] M. Röβler, I.O.-C. and C. Research, undefined, Investigations on the relationship between porosity, structure and strength of hydrated portland cement pastes I, in: Effect of Porosity, Elsevier, 1985 (n.d.), https://www.sciencedirect.com/science/article/pii/0008884685900444. (Accessed 5 November 2021).
[39] M.M. Ali, K.S. Moon, Advances in structural systems for tall buildings: emerging developments for contemporary urban giants, Buildings 8 (2018) 104, https://doi.org/10.3390/BUILDINGS8080104, 8 (2018) 104.
[40] I.B. Topçu, B. Işikdağ, Effect of expanded perlite aggregate on the properties of lightweight concrete, J. Mater. Process. Technol. 204 (2008) 34–38, https://doi.org/10.1016/J.JMATPROTEC.2007.10.052.
[41] Z.M. Yaseen, R.C. Deo, A. Hilal, A.M. Abd, L.C. Bueno, S. Salcedo-Sanz, M. L. Nehdi, Predicting compressive strength of lightweight foamed concrete using extreme learning machine model, Adv. Eng. Software 115 (2018) 112–125, https://doi.org/10.1016/J.ADVENGSOFT.2017.09.004.
[42] M. Mydin, Y.W. C, B. Materials, undefined, Mechanical Properties of Foamed Concrete Exposed to High Temperatures, Elsevier, 2012 (n.d.), https://www.sciencedirect.com/science/article/pii/S0950061811003308. (Accessed 6 November 2021).
[43] P. Tikalsky, J. Pospisil, W.M. C, concrete research, undefined, A Method for Assessment of the Freeze–Thaw Resistance of Preformed Foam Cellular Concrete, Elsevier, 2004 (n.d.), https://www.sciencedirect.com/science/article/pii/S0008884603003909. (Accessed 6 November 2021).
[44] L.B. Yen, Study of Water Ingress into Foamed Concrete, ScholarBank@NUS Repository, 2007, p. 177. https://scholarbank.nus.edu.sg/handle/10635/23133. (Accessed 30 December 2021).
[45] N. Narayanan, K.R. C, C. Research, undefined, Microstructural Investigations on Aerated Concrete, Elsevier, 2000 (n.d.), https://www.sciencedirect.com/science/article/pii/S000884600000199X. (Accessed 6 November 2021).
[46] E. Nambiar, K.R. C, concrete research, undefined, Air-void characterisation of foam concrete, Elsevier, 2007 (n.d. https://www.sciencedirect.com/science/article/pii/S0008884606002699. (Accessed 6 November 2021).
[47] M. Kozłowski, M. Kadela, A.K.-P. Engineering, undefined, Fracture Energy of Foamed Concrete Based on Three-point Bending Test on Notched Beams, Elsevier, 2015 (n.d.), https://www.sciencedirect.com/science/article/pii/S187770581501111X. (Accessed 6 November 2021).
[48] H. Sun, A. Gong, Y. Peng, X. Wang, The Study of Foamed Concrete with Polypropylene Fiber and High Volume Fly Ash, Trans Tech Publ, 2011 (n.d.), https://www.scientific.net/AMM.90-93.1039. (Accessed 6 November 2021).
[49] M. Jones, A.M. C, concrete research, undefined, Heat of Hydration in Foamed Concrete: Effect of Mix Constituents and Plastic Density, Elsevier, 2006 (n.d.), https://www.sciencedirect.com/science/article/pii/S0008884606000068. (Accessed 6 November 2021).
[50] Z. Pan, F. Hiromi, T. Wee, Preparation of high performance foamed concrete from cement, sand and mineral admixtures, J. Wuhan Univ. Technol.-Materials Sci. Ed. 22 (2007) 295–298, https://doi.org/10.1007/s11595-005-2295-4.
[51] E.P. Kearsley, P.J. Wainwright, The effect of high fly ash content on the compressive strength of foamed concrete, Cement Concr. Res. 31 (2001) 105–112, https://doi.org/10.1016/S0008-8846(00)00430-0.
[52] K. Ramamurthy, E. Nambiar, G.R. C, concrete, undefined, A Classification of Studies on Properties of Foam Concrete, Elsevier, 2009 (n.d. https://www.sciencedirect.com/science/article/pii/S0958946509000638. (Accessed 5 November 2021).
[53] A. Hilal, N. Thom, A.D. C, B. Materials, undefined, On Void Structure and Strength of Foamed Concrete Made Without/with Additives, Elsevier, 2015 (n.d.), https://www.sciencedirect.com/science/article/pii/S0950061815003724. (Accessed 5 November 2021).
[54] E. Kearsley, P.W. C, The effect of high fly ash content on the compressive strength of foamed concrete, in: Concrete Research, Undefined, Elsevier, 2001 (n.d.), https://www.sciencedirect.com/science/article/pii/S0008884600004300. (Accessed 5 November 2021).
[55] M. Nehdi, Y. Djebbar, A.K.-M. Journal, undefined, Neural Network Model for Preformed-Foam Cellular Concrete, Researchgate.Net., 2001. https://www.researchgate.net/profile/Moncef-Nehdi/publication/279573475_Neural_network_model_for_preformed-foam_cellular_concrete/links/575c39e008aed884621337d0/Neural-network-model-for-preformed-foam-cellular-concrete.pdf. (Accessed 6 November 2021), 2001.
[56] N. Narayanan, K.R. C, C. composites, undefined, Structure and Properties of Aerated Concrete: a Review, Elsevier, 2000 (n.d.), https://www.sciencedirect.com/science/article/pii/S0958946500000160. (Accessed 6 November 2021).
[57] Z. Pan, F. Hiromi, T.W.-J. of W.U. of Technology-Mater, undefined, Preparation of High Performance Foamed Concrete from Cement, Sand and Mineral Admixtures, vol. 22, Springer, 2007, pp. 295–298, https://doi.org/10.1007/s11595-005-2295-4, 2007.
[58] T. Nguyen, A. Kashani, T. Ngo, S. Bordas, Deep neural network with high-order neuron for the prediction of foamed concrete strength, Comput. Aided Civ. Infrastruct. Eng. 34 (2019) 316–332, https://doi.org/10.1111/MICE.12422.
[59] B. Kiani, A.H. Gandomi, S. Sajedi, R.Y. Liang, New formulation of compressive strength of preformed-foam cellular concrete: an evolutionary approach, J. Mater. Civ. Eng. 28 (2016), 04016092, https://doi.org/10.1061/(ASCE)MT.1943-5533.0001602.
[60] M. Nehdi, Y. Djebbar, A. Khan, Neural network model for preformed-foam cellular concrete, Materials J. 98 (2001) 402–409, https://doi.org/10.14359/10730.
[61] J. Chou, A.P. C, B. Materials, undefined, Enhanced Artificial Intelligence for Ensemble Approach to Predicting High Performance Concrete Compressive Strength, Elsevier, 2013 (n.d.), https://www.sciencedirect.com/science/article/pii/S0950061813008088. (Accessed 6 November 2021).
[62] D. Falliano, D. de Domenico, G. Ricciardi, E. Gugliandolo, Experimental investigation on the compressive strength of foamed concrete: effect of curing conditions, cement type, foaming agent and dry density, Construct. Build. Mater. 165 (2018) 735–749, https://doi.org/10.1016/J.CONBUILDMAT.2017.12.241.
[63] J. He, Q. Gao, X. Song, X. Bu, J. He, Effect of foaming agent on physical and mechanical properties of alkali-activated slag foamed concrete, Construct. Build. Mater. 226 (2019) 280–287, https://doi.org/10.1016/J.CONBUILDMAT.2019.07.302.
[64] C.D. Welker, M.A. Welker, M.F. Welker, M.A. Justman, R.S. Hendricksen, US6153005A - Foamed Concrete Composition and Process - Google Patents, USPTO, 2000. https://patents.google.com/patent/US6153005A/en. (Accessed 10 April 2022).
[65] F.H. Chiew, C.K. Ng, K.C. Chai, K.M. Tay, A fuzzy adaptive resonance theory-based model for mix proportion estimation of high-performance concrete, Comput. Aided Civ. Infrastruct. Eng. 32 (2017) 772–786, https://doi.org/10.1111/MICE.12288.
[66] A. Imam, B.A. Salami, T.A. Oyehan, Predicting the compressive strength of a quaternary blend concrete using Bayesian regularized neural network, Https://Doi.Org/10.1080/24705314.2021.1892572. 6, https://doi.org/10.1080/24705314.2021.1892572, 2021, 237-246.
[67] B.A. Salami, T. Olayiwola, T.A. Oyehan, I.A. Raji, Data-driven model for ternary-blend concrete compressive strength prediction using machine learning approach, Construct. Build. Mater. 301 (2021), 124152, https://doi.org/10.1016/J.CONBUILDMAT.2021.124152.
[68] M. Shariati, D.J. Armaghani, M. Khandelwal, J. Zhou, M. Khorami, Assessment of longstanding effects of fly ash and silica fume on the compressive strength of concrete using extreme learning machine and artificial neural network, J. Adv. Eng. Computation 5 (2021) 50–74, https://doi.org/10.25073/JAEC.202151.308.
[69] M. Shariati, M.S. Mafipour, P. Mehrabi, A. Shariati, A. Toghroli, N.T. Trung, M.N. A. Salih, A novel approach to predict shear strength of tilted angle connectors using artificial intelligence techniques, Eng. Comput. 37 (2021) 2089, https://doi.org/10.1007/S00366-019-00930-X, 2109.
[70] H.A. Algaifi, S.A. Bakar, R. Alyousef, A.R.Mohd Sam, A.S. Alqarni, M.H. W. Ibrahim, S. Shahidan, M. Ibrahim, B.A. Salami, H.A. Algaifi, S.A. Bakar, R. Alyousef, A.R.Mohd Sam, A.S. Alqarni, M.H.W. Ibrahim, S. Shahidan, M. Ibrahim, B.A. Salami, Machine learning and RSM models for prediction of compressive strength of smart bio-concrete, Smart Struct. Syst. 28 (2021) 535, https://doi.org/10.12989/SSS.2021.28.4.535.
[71] H.A. Algaifi, A.S. Alqarni, R. Alyousef, S.A. Bakar, M.H.W. Ibrahim, S. Shahidan, M. Ibrahim, B.A. Salami, Mathematical prediction of the compressive strength of bacterial concrete using gene expression programming, Ain Shams Eng. J. (2021), https://doi.org/10.1016/J.ASEJ.2021.04.008.
[72] M. Shariati, M.S. Mafipour, P. Mehrabi, A. Bahadori, Y. Zandi, M.N.A. Salih, H. Nguyen, J. Dou, X. Song, S. Poi-Ngian, Application of a hybrid artificial neural network-particle swarm optimization (ANN-PSO) model in behavior prediction of channel shear connectors embedded in normal and high-strength concrete, Appl. Sci. 9 (2019) 5534, https://doi.org/10.3390/APP9245534, 9 (2019) 5534.
[73] M. Shariati, M.S. Mafipour, P. Mehrabi, M. Ahmadi, K. Wakil, N.T. Trung, A. Toghroli, Prediction of concrete strength in presence of furnace slag and fly ash using Hybrid ANN-GA (Artificial Neural Network-Genetic Algorithm), Smart Struct. Syst. 25 (2020) 183–195, https://doi.org/10.12989/SSS.2020.25.2.183.
[74] B.A. Salami, S.M. Rahman, T.A. Oyehan, M. Maslehuddin, S.U. al Dulaijan, Ensemble machine learning model for corrosion initiation time estimation of embedded steel reinforced self-compacting concrete, Measurement 165 (2020), 108141, https://doi.org/10.1016/j.measurement.2020.108141.
[75] J. Zhang, Y. Huang, G. Ma, Y. Yuan, B. Nener, Automating the mixture design of lightweight foamed concrete using multi-objective firefly algorithm and support vector regression, Cement Concr. Compos. 121 (2021), 104103, https://doi.org/10.1016/J.CEMCONCOMP.2021.104103.
[76] A.-D. Pham, N.-T. Ngo, Q.-T. Nguyen, N.-S. Truong, Hybrid machine learning for predicting strength of sustainable concrete, Soft Comput. 24 (2020) 14965–14980, https://doi.org/10.1007/S00500-020-04848-1, 19. 24 (2020).
[77] D. van Dao, H.-B. Ly, H.-L.T. Vu, T.-T. Le, B.T. Pham, Investigation and optimization of the C-ANN structure in predicting the compressive strength of

foamed concrete, Materials 13 (2020) 1072, https://doi.org/10.3390/MA13051072, 13 (2020) 1072.
[78] M.N. Amin, M. Iqbal, K. Khan, M.G. Qadir, F.I. Shalabi, A. Jamal, Ensemble tree-based approach towards flexural strength prediction of FRP reinforced concrete beams, Polymers 14 (2022) 1303, https://doi.org/10.3390/POLYM14071303, 14 (2022) 1303.
[79] F.I. Syed, T. Muther, A.K. Dahaghi, S. Negahban, AI/ML assisted shale gas production performance evaluation, J. Pet. Explor. Prod. Technol. 11 (2021) 3509–3519, https://doi.org/10.1007/S13202-021-01253-8/FIGURES/7.
[80] R.S. Faradonbeh, M. Hasanipanah, H.B. Amnieh, D.J. Armaghani, M. Monjezi, Development of GP and GEP models to estimate an environmental issue induced by blasting operation, Environ. Monit. Assess. 190 (2018) 1–15, https://doi.org/10.1007/S10661-018-6719-Y/FIGURES/10.
[81] M. Iqbal, D. Zhang, F.E. Jalal, Durability evaluation of GFRP rebars in harsh alkaline environment using optimized tree-based random forest model, J. Ocean Eng. Sci. (2021), https://doi.org/10.1016/J.JOES.2021.10.012.
[82] M.R. Jones, A. McCarthy, Preliminary views on the potential of foamed concrete as a structural material, Mag. Concr. Res. 57 (2005) 21–31, https://doi.org/10.1680/MACR.2005.57.1.21.
[83] Z. Pan, F. Hiromi, T. Wee, Preparation of high performance foamed concrete from cement, sand and mineral admixtures, J. Wuhan Univ. Technol.-Materials Sci. Ed. 22 (2007) 295–298, https://doi.org/10.1007/S11595-005-2295-4, 2. 22 2007.
[84] T. Nguyen, A. Kashani, T. Ngo, S. Bordas, Deep neural network with high-order neuron for the prediction of foamed concrete strength, Comput. Aided Civ. Infrastruct. Eng. 34 (2019) 316–332, https://doi.org/10.1111/mice.12422.
[85] B. Kiani, A.H. Gandomi, S. Sajedi, R.Y. Liang, New formulation of compressive strength of preformed-foam cellular concrete: an evolutionary approach, J. Mater. Civ. Eng. 28 (2016), 04016092, https://doi.org/10.1061/(ASCE)MT.1943-5533.0001602.
[86] S. Asadzadeh, S. Khoshbayan, Multi-objective optimization of influential factors on production process of foamed concrete using Box-Behnken approach, Construct. Build. Mater. 170 (2018) 101–110, https://doi.org/10.1016/J.CONBUILDMAT.2018.02.189.
[87] A.M. Abd, S.M. Abd, Modelling the strength of lightweight foamed concrete using support vector machine (SVM), Case Stud. Constr. Mater. 6 (2017) 8–15, https://doi.org/10.1016/J.CSCM.2016.11.002.
[88] P.G. Asteris, A.D. Skentou, A. Bardhan, P. Samui, K. Pilakoutas, Predicting concrete compressive strength using hybrid ensembling of surrogate machine learning models, Cement Concr. Res. 145 (2021), 106449, https://doi.org/10.1016/J.CEMCONRES.2021.106449.
[89] A. Hajimohammadi, T. Ngo, P. Mendis, T. Nguyen, A. Kashani, J.S.J. van Deventer, Pore characteristics in one-part mix geopolymers foamed by H2O2: the impact of mix design, Mater. Des. 130 (2017) 381–391, https://doi.org/10.1016/J.MATDES.2017.05.084.
[90] A. Hajimohammadi, T. Ngo, P. Mendis, J. Sanjayan, Regulating the chemical foaming reaction to control the porosity of geopolymer foams, Mater. Des. 120 (2017) 255–265, https://doi.org/10.1016/J.MATDES.2017.02.026.
[91] R. Othman, R.P. Jaya, K. Muthusamy, M. Sulaiman, Y. Duraisamy, M.M.A. B. Abdullah, A. Przybył, W. Sochacki, T. Skrzypczak, P. Vizureanu, A.V. Sandu, Relation between density and compressive strength of foamed concrete, Materials 14 (2021), https://doi.org/10.3390/MA14112967.
[92] Y. Fu, X. Wang, L. Wang, Y. Li, Foam concrete: a state-of-the-art and state-of-the-practice review, Adv. Mater. Sci. Eng. (2020) 2020, https://doi.org/10.1155/2020/6153602.
[93] T.H. Wee, S.B. Daneti, T. Tamilselvan, Effect of w/c ratio on air-void system of foamed concrete and their influence on mechanical properties, Http://Dx.Doi.Org/10.1680/Macr.2011.63.8.583. 63, https://doi.org/10.1680/MACR.2011.63.8.583, 2015, 583-595.
[94] M.S. Hamidah, I. Azmi, M.R.A. Ruslan, K. Kartini, N.M. Fadhil, Optimisation of foamed concrete mix of different sand-cement ratio and curing conditions, in: Proceedings of the International Conference on the Use of Foamed Concrete in Construction, 2005, pp. 37–44, https://doi.org/10.1680/UOFCIC.34068.0005.
[95] A.H. Gandomi, G.J. Yun, A.H. Alavi, An evolutionary approach for modeling of shear strength of RC deep beams, Materials and Structures/Materiaux et Constructions 46 (2013) 2109–2119, https://doi.org/10.1617/S11527-013-0039-Z/TABLES/4.
[96] A.H. Gandomi, S.K. Babanajad, A.H. Alavi, Y. Farnam, Novel approach to strength modeling of concrete under triaxial compression, J. Mater. Civ. Eng. 24 (2012) 1132–1143, https://doi.org/10.1061/(ASCE)MT.1943-5533.0000494.
[97] R. Poli, J. Koza, Genetic Programming, Search Methodologies: Introductory Tutorials in Optimization and Decision Support Techniques, second ed., 2014, pp. 143–185, https://doi.org/10.1007/978-1-4614-6940-7_6.
[98] M. Saridemir, Genetic programming approach for prediction of compressive strength of concretes containing rice husk ash, Construct. Build. Mater. 24 (2010) 1911–1919, https://doi.org/10.1016/J.CONBUILDMAT.2010.04.011.
[99] F. Özcan, Gene expression programming based formulations for splitting tensile strength of concrete, Construct. Build. Mater. 26 (2012) 404–410, https://doi.org/10.1016/J.CONBUILDMAT.2011.06.039.
[100] M.A. Khan, A. Zafar, A. Akbar, M.F. Javed, A. Mosavi, Application of gene expression programming (GEP) for the prediction of compressive strength of geopolymer concrete, Materials 14 (2021) 1–23, https://doi.org/10.3390/MA14051106.
[101] F.A.N. Silva, J.M.P.Q. Delgado, R.S. Cavalcanti, A.C. Azevedo, A.S. Guimarães, A. G.B. Lima, Use of nondestructive testing of ultrasound and artificial neural networks to estimate compressive strength of concrete, Buildings 11 (2021) 44, https://doi.org/10.3390/BUILDINGS11020044, 11 (2021) 44.
[102] H. Madani, Mohammad Kooshafar, M. Emadi, Compressive strength prediction of nanosilica-incorporated cement mixtures using adaptive neuro-fuzzy inference system and artificial neural network models, Pract. Period. Struct. Des. Construct. 25 (2020), 04020021, https://doi.org/10.1061/(ASCE)SC.1943-5576.0000499.
[103] M. Kovačević, S. Lozančić, E.K. Nyarko, M. Hadzima-nyarko, Modeling of compressive strength of self-compacting rubberized concrete using machine learning, Materials 14 (2021) 4346, https://doi.org/10.3390/MA14154346, 14 (2021) 4346.
[104] P. Neira, L. Bennun, M. Pradena, J. Gomez, Prediction of concrete compressive strength through artificial neural network, Gradjevinar 72 (2020) 585–592, https://doi.org/10.14256/JCE.2438.2018.
[105] T. Mehmannavaz, V. Khalilikhorram, S.M. Sajjadi, M. Samadi, Presenting an appropriate neural network for optimal mix design of roller compacted concrete dams, Res. J. Appl. Sci. Eng. Technol. 7 (2014) 1872, https://doi.org/10.19026/RJASET.7.475. –1877.
[106] M.I. Khan, Predicting properties of high performance concrete containing composite cementitious materials using artificial neural networks, Autom. ConStruct. 22 (2012) 516–524, https://doi.org/10.1016/J.AUTCON.2011.11.011.
[107] Z.H. Duan, S.C. Kou, C.S. Poon, Prediction of compressive strength of recycled aggregate concrete using artificial neural networks, Construct. Build. Mater. 40 (2013) 1200–1206, https://doi.org/10.1016/J.CONBUILDMAT.2012.04.063.
[108] K.C. Onyelowe, M. Iqbal, F.E. Jalal, M.E. Onyia, I.C. Onuoha, Application of 3-algorithm ANN programming to predict the strength performance of hydrated-lime activated rice husk ash treated soil, Multiscale and Multidisciplinary Modeling, Experiments and Design 4 (2021) 259–274, https://doi.org/10.1007/s41939-021-00093-7.
[109] R.S. Faradonbeh, M. Hasanipanah, H.B. Amnieh, D.J. Armaghani, M. Monjezi, Development of GP and GEP models to estimate an environmental issue induced by blasting operation, Environ. Monit. Assess. 190 (2018), https://doi.org/10.1007/s10661-018-6719-y.
[110] M. Khandelwal, R. Shirani Faradonbeh, M. Monjezi, D.J. Armaghani, M.Z.B. A. Majid, S. Yagiz, Function development for appraising brittleness of intact rocks using genetic programming and non-linear multiple regression models, Eng. Comput. 33 (2017) 13–21, https://doi.org/10.1007/s00366-016-0452-3.
[111] C. Ferreira, Gene expression programming in problem solving, Soft Computing and Industry (2002) 635–653, https://doi.org/10.1007/978-1-4471-0123-9_54.
[112] C. Ferreira, Gene Expression Programming Mathematical Modeling by an Artificial Intelligence, vol. 21, Springer, 2006, p. 478.
[113] J. Brownlee, Clever Algorithms - Nature-Inspired Programming Recipes, Jason Brownlee, 2011. http://www.cleveralgorithms.com.
[114] G. Giakoumelis, D. Lam, Axial capacity of circular concrete-filled tube columns, J. Constr. Steel Res. 60 (2004) 1049–1068, https://doi.org/10.1016/j.jcsr.2003.10.001.
[115] K. Sakino, H. Nakahara, S. Morino, I. Nishiyama, Behavior of centrally loaded concrete-filled steel-tube short columns, J. Struct. Eng. 130 (2004) 180–188, https://doi.org/10.1061/(asce)0733-9445(2004)130:2(180).
[116] E.M. Golafshani, A. Behnood, M. Arashpour, Predicting the compressive strength of normal and high-performance concretes using ANN and ANFIS hybridized with grey wolf optimizer, Construct. Build. Mater. 232 (2020), 117266, https://doi.org/10.1016/j.conbuildmat.2019.117266.
[117] I.O. Alade, A. Bagudu, T.A. Oyehan, M.A.A. Rahman, T.A. Saleh, S.O. Olatunji, Estimating the refractive index of oxygenated and deoxygenated hemoglobin using genetic algorithm – support vector regression model, Comput. Methods Progr. Biomed. 163 (2018) 135–142, https://doi.org/10.1016/j.cmpb.2018.05.029.
[118] M.F. Iqbal, Q. feng Liu, I. Azim, X. Zhu, J. Yang, M.F. Javed, M. Rauf, Prediction of mechanical properties of green concrete incorporating waste foundry sand based on gene expression programming, J. Hazard Mater. 384 (2020), 121322, https://doi.org/10.1016/j.jhazmat.2019.121322.
[119] A.H. Gandomi, D.A. Roke, Assessment of artificial neural network and genetic programming as predictive tools, Adv. Eng. Software 88 (2015) 63–72, https://doi.org/10.1016/j.advengsoft.2015.05.007.
[120] A. Gholampour, A.H. Gandomi, T. Ozbakkaloglu, New formulations for mechanical properties of recycled aggregate concrete using gene expression programming, Construct. Build. Mater. 130 (2017) 122–145, https://doi.org/10.1016/j.conbuildmat.2016.10.114.
[121] S. Soleimani, S. Rajaei, P. Jiao, A. Sabz, S. Soheilinia, New prediction models for unconfined compressive strength of geopolymer stabilized soil using multi-gen genetic programming, Measurement, J. Int. Measurement Confederation 113 (2018) 99–107, https://doi.org/10.1016/j.measurement.2017.08.043.
[122] Y. Erzin, Artificial neural networks approach for swell pressure versus soil suction behaviour, Can. Geotech. J. 44 (2007) 1215–1223, https://doi.org/10.1139/T07-052.
[123] W. el Ansari, C.J. Phillips, Interprofessional collaboration: a stakeholder approach to evaluation of voluntary participation in community partnerships, J. Interprof. Care 15 (2001) 351–368, https://doi.org/10.1080/13561820120080481.
[124] Y. Agematsu, I. Ikarashi, Y. Furuyama, N. Kobayashi, K. Barada, K. Tauchi, A new visual method for evaluating multiple data (diagnostic radar chart) in general toxicological study, J. Toxicol. Sci. 18 (1993) 133–142, https://doi.org/10.2131/jts.18.3_133.
[125] N. Tugcu, A. Ladiwala, C.M. Breneman, S.M. Cramer, Identification of chemically selective displacers using parallel batch screening experiments and quantitative structure efficacy relationship models, Anal. Chem. 75 (2003) 5806–5816, https://doi.org/10.1021/ac0341564.